MOLECULAR ECOLOGY

A functional transcriptomics analysis in the relict marsupial Dromiciops gliroides reveals adaptive regulation of protective functions during hibernation

Journal:	*Molecular Ecology*
Manuscript ID	MEC-18-0482.R1
Manuscript Type:	Original Article
Date Submitted by the Author:	05-Aug-2018
Complete List of Authors:	Nespolo, Roberto; Universidad Austral de Chile, Instituto de Ciencias Ambientales y Evolutivas Gaitán-Espitia, Juan Diego; Universidad Austral de Chile, Instituto de Ciencias Ambientales y Evolutivas Quintero-Galvis, Julian; Universidad Austral de Chile Fernandez, Fernanda; Universidad Austral de Chile Silva, Andrea; Universidad Austral de Chile Molina, Cristian; Universidad Austral de Chile Storey, Kenneth; Carleton University, Institute of Biochemistry & Department of Biology Bozinovic, Francisco; Pontificia Universidad Catolica de Chile
Keywords:	Transcriptomics, Comparative Physiology, hibernation, marsupials, Dromiciops

A functional transcriptomics analysis in the relict marsupial *Dromiciops gliroides* reveals adaptive regulation of protective functions during hibernation

Roberto F. Nespolo[1,2,3*], *Juan Diego Gaitan-Espitia*[4,5], *Julian F. Quintero-Galvis*[1], *Fernanda V. Fernandez*[6], *Andrea X. Silva*[7], *Cristian Molina*[7], *Kenneth B. Storey*[8], *Francisco Bozinovic*[2].

[1]*Instituto de Ciencias Ambientales y Evolutivas, Facultad de Ciencias, Universidad Austral de Chile, Valdivia, Chile.*

[2]*Center of Applied Ecology and Sustainability (CAPES), Facultad de Ciencias Biológicas, Universidad Católica de Chile, Santiago 6513677, Chile.*

[3]*Millennium Institute for Integrative Systems and Synthetic Biology (MIISSB), Santiago, Chile.*

[4] *The Swire Institute of Marine Science and School of Biological Sciences, The University of Hong Kong, Hong Kong SAR, China.*

[5] *CSIRO Oceans & Atmosphere, GPO Box 1538, Hobart 7001, TAS, Australia.*

[6]*Instituto de Fisiología, Facultad de Medicina, Universidad Austral de Chile.*

[7]*AUSTRALomics, Facultad de Ciencias, Universidad Austral de Chile.*

[8]*Department of Biology and Institute of Biochemistry, Carleton University, 1125 Colonel By Drive, Ottawa, Ontario K1S 5B6, Canada.*

*Corresponding author

robertonespolorossi@gmail.com

Abstract

The small South American marsupial, *Dromiciops gliroides*, known as the missing link between the American and the Australian marsupials, is one of the few South American mammals known to hibernate. Expressing both daily torpor and seasonal hibernation, this species may provide crucial information about the mechanisms and the evolutionary origins of marsupial hibernation. Here we compared torpid and active individuals, applying high-throughput sequencing technologies (RNA-seq) to profile gene expression in three *D. gliroides* tissues and determine whether hibernation induces tissue-specific differential gene expression. We found 566 transcripts that were significantly up-regulated during hibernation (369 in brain, 147 in liver and 50 in skeletal muscle) and 339 that were down-regulated (225 in brain, 79 in liver and 35 in muscle). The proteins encoded by these differentially expressed genes orchestrate multiple metabolic changes during hibernation, such as inhibition of angiogenesis, prevention of muscle disuse atrophy, fuel switch from carbohydrate to lipid metabolism, protection against reactive oxygen species and repair of damaged DNA. According to the global enrichment analysis, brain cells seem to differentially regulate a complex array of biological functions (e.g., cold sensitivity, circadian perception, stress response); whereas liver and muscle cells prioritize fuel switch and heat production for rewarming. Interestingly, transcripts of thioredoxin interacting protein (*TXNIP*), a potent antioxidant, were significantly overexpressed during torpor in all three tissues. These results suggest that marsupial hibernation is a controlled process where selected metabolic pathways show adaptive modulation that can help to maintain homeostasis and enhance cytoprotection in the hypometabolic state.

Key words: hibernation, functional genomics, marsupials, adaptation, Dromiciops, RNA-seq.

1. Introduction

Endothermic animals (i.e., birds and mammals) produce metabolic heat in their bodies in a way that allows them to maintain a near-constant body temperature at values that are typically well above ambient temperature. This is an extravagant economy that requires these animals to maintain elevated energy budgets and spend a large part of their resources on basic maintenance. However, the benefits are large and allow endotherms to remain active in cold environments or travel long distances due to their high aerobic capacity, the only way to sustain long periods of activity (Koteja, 2004; Nespolo, Bacigalupe, Figueroa, Koteja, & Opazo, 2011). An adaptive strategy to ameliorate the high cost of endothermy is torpor, an energy-saving mechanism used by many small mammal and bird species, that involves a temporal interruption of endothermy that happens during cold periods (Boyer & Barnes, 1999; Ruf & Geiser, 2015). During torpor episodes, which can occur daily or seasonally (seasonal torpor is also known as hibernation, see reviews in Boyles et al., 2013; Ruf & Geiser, 2015), most normal biological functions are suppressed for periods ranging from overnight to several weeks. Animals show strong suppression of metabolic rate (often to values just 1-10% of active levels)(Ruf & Geiser, 2015), a decrease in body temperature to near ambient values, and experience reductions in most physiological processes (e.g. strongly reduced heart beat and breathing rates). In these hypometabolic states, energy is re-allocated to some pathways that maintain organ function, whereas other processes are suppressed or interrupted. For instance, the brain, an organ that cannot be shut down without serious damage, receives about 10% of its normal perfusion during torpor but maintains neural activity, especially in the hypothalamus (Schwartz, Hampton, & Andrews, 2013). The liver, the metabolic center of the body, is also important during torpor as this organ processes nutrients, detoxifies reactive oxygen species (ROS) and disposes toxic

products, and produces multiple proteins and fuels for export to other tissues (Hadj-Moussa et al., 2016). Another important tissue, that shows reduced perfusion during torpor, is skeletal muscle. This tissue cannot be damaged as it is crucial for rewarming the body during arousal from hibernation (Hindle, Karimpour-Fard, Epperson, Hunter, & Martin, 2011).

The state of suspended animation characterizing torpor and hibernation (i.e., the "hibernation phenotype", (Faherty, Villanueva-Canas, Klopfer, Alba, & Yoder, 2016) entails important risks for cells and tissues. A wealth of knowledge obtained from placental mammals, for instance, has shown that torpor increases the risk of cardiac arrest and since blood perfusion to peripheral organs can be reduced, tissues can become hypoxic and ischemic. This in turn increases the risk of oxidative damage especially resulting from a massive production of ROS during arousal (Fons, Sender, Peters, & Jurgens, 1997; Rouble, Tessier, & Storey, 2014; Schwartz et al., 2013; van Breukelen, Krumschnabel, & Podrabsky, 2010). In the brain for instance, a reversible loss of synapses occurs, which reduces metabolic activity and helps to avoid the risk of neuronal death during torpor (Andrews, 2004 ; Schwartz et al., 2013). In skeletal muscle, adaptive mechanisms minimizing muscular disuse atrophy during torpor include differential regulation of genes related to protein biosynthesis and focal adhesion, which helps to maintain muscle integrity and contractibility (Andres-Mateos et al., 2012; Fedorov et al., 2014; Hadj-Moussa et al., 2016). Several detailed studies, all performed in placental mammals (reviewed in Andrews, 2004; Carey, Andrews, & Martin, 2003; Morin & Storey, 2009; Villanueva-Canas, Faherty, Yoder, & Alba, 2014) have revealed that these changes involve transcriptional (gene-expression), post-transcriptional (non-coding RNA), translational (protein synthesis) and post-translational (reversible protein modification) changes assisting these pro-survival

measures. Here we present a case of massive transcriptional changes, many of them with adaptive significance, occurring in an hibernating species of marsupial.

Marsupials shared a last common ancestor with placental mammals approximately 160 million years ago (Graves & Renfree, 2013; Renfree, 1981) and since then, they have diversified into a wide range of ecological niches, especially after the colonization of Australia in the late-Cretaceous (Mitchell et al., 2014). Multiple small marsupial species exhibit torpor, which represents an evolutionary convergence with placental mammals (see Ruf & Geiser, 2015; Turner, Warnecke, Kortner, & Geiser, 2012). However, the underlying metabolic origins and patterns of marsupial hibernation are unclear. We know of three published studies describing some functional aspects of marsupial hibernation (Franco, Contreras, & Nespolo, 2013; Hadj-Moussa et al., 2016; Malan, 2010), which indicate some similarities with placental mammals (e.g., immunity suppression, mechanisms avoiding muscle atrophy, fuel switch to fat metabolism) but also some differences (e.g., a thermogenic role of the liver for rewarming and maintenance of the Akt metabolic pathway during torpor in the liver; Hadj-Moussa et al., 2016; Luu et al., 2018a; Villarin, Schaeffer, Markle, & Lindstedt, 2003). In this study, we used RNA-seq to analyze genomic-wide expression patterns of central and peripheral organs in the South American marsupial *Dromiciops gliroides*. This species is considered a "relict" mammal (sensu Habel, Assman, Schmidtt, & Avise, 2010) as it belongs to Microbiotheria, a formerly diverse group that diverged from Didelphimorphia (American marsupials) about 70 million years ago (MYA) and gave rise to Australidelphia, the large clade of Australian marsupials (Graves & Renfree, 2013; Mitchell et al., 2014). All Microbiotherids are extinct, excepting for *D. gliroides* (Palma & Spotorno, 1999).

According to Bozinovic et al. (2004), *D. gliroides* is one of the few South American mammals that exhibit hibernation (=seasonal torpor, see also Geiser & Martin, 2013), but it also exhibits short torpor episodes during summer (i.e., daily torpor) (Bozinovic, Ruiz, & Rosenmann, 2004; Nespolo, Verdugo, Cortes, & Bacigalupe, 2010). By the use of torpor, *D. gliroides* can save up to 60% of the energy that would otherwise be needed during the cold period. Previous work on *D. gliroides* suggested that torpor is associated with metabolic rate reductions of about 90% (Nespolo et al., 2010). During daily torpor episodes in *D. gliroides*, a drastic redistribution of blood in the body induces anemia, leukopenia, muscle atrophy and inflammation (Franco et al., 2013).

The apparently random patterns of torpor that *D. gliroides* exhibit were formerly interpreted as acute, uncontrolled responses to cold (Nespolo et al., 2010). However, a number of recent discoveries have changed this view. For instance, *D. gliroides* seems to anticipate the cold season as a response to photoperiodic changes and thermal acclimation (Franco, Contreras, Place, Bozinovic, & Nespolo, 2017). In addition, several torpor-regulation mechanisms were described in this species, including differential expression microRNAs (Hadj-Moussa et al., 2016), implementation of the stress response through MAPK signaling (Luu et al., 2018b; Wijenayake et al., 2018a), reorganization of fuel use (Wijenayake et al., 2018b), and partial suppression of protein synthesis (Luu et al., 2018a). Here we present a comprehensive transcriptomics analysis of torpid *D. gliroides*, providing the first explicit description of differentially regulated metabolic pathways of marsupial hibernation.

2. Methods

2.1 Animal collection and laboratory treatment

D. gliroides is one of the four marsupial species of Chile; it is an omnivorous, nocturnal, opossum-like mammal with arboreal adaptations (i.e., opposable thumbs, prehensile tail and eyes in frontal plane) (Hershkovitz, 1999). This species is strongly associated with the temperate rainforest, where temperatures fluctuate between 5 and 25ºC (Franco et al., 2017). In this ecosystem, we captured thirteen adult *D. gliroides* (7 males; 6 females), particularly in the Southern part of Valdivia, Chile (39°48′S, 73°14′W; 9 m.a.s.l.) during the austral summer (January-February) in 2014, using Tomahawk traps located in trees 1m above ground, baited with bananas and yeast. Upon capture, individuals were immediately transported to the laboratory where they were housed in plastic cages of 45x30x20 cm^3 with 2 cm of bedding. All individuals were maintained in a climate controlled chamber (PiTec Instruments, Chile) at 20±1°C and with a 12 h: 12 h photoperiod for two weeks. Animals were fed a mix of mealworms, fruits, and water ad libitum. After two weeks of acclimation, and after checking that each animal had increased body mass, individuals were randomly assigned to two groups: torpor (3 males, 4 females) and active controls (3 males, 3 females). Active animals were sampled from the above conditions. To induce torpor, and to avoid any injury, animals were subjected to a gradual decrease of ambient temperature (−1 °C every 20 min) until 10 °C was reached (photoperiod was maintained as initially). To minimize animal disturbance during the experimental trials, torpor incidence was verified by visual observation several times a day between 09:00–17:00. In this species torpor can be easily identified: animals are not responsive when the cage is gently moved and breathing frequency is below three breaths per minute. After declaring torpor for a given individual, the animal was continuously monitored by visual inspection every four hours, during four consecutive days to ensure that torpor was sustained; and individuals were then euthanized. Euthanasia followed protocols approved

by the Committee on the Ethics of Animal Experiments of the Universidad Austral de Chile. Tissue samples were excised in less than a minute and immediately frozen in liquid nitrogen. All animals capture, handling and maintenance procedures followed the guidelines of the American Society of Mammalogists (Gannon, Sikes, & Comm, 2007) and were authorized by the Chilean Agriculture and Livestock Bureau (SAG: Servicio Agrícola y Ganadero de Chile, permit No. 1054/2014 and 1118/2015).

2.2 RNA extraction, cDNA library construction and sequencing

Total RNA was extracted from brain, liver and skeletal muscle from the hind leg (thigh) of each animal using the NucleoSpin RNA II Macherey Nagel kit (Bethlehem, PA, USA) and additional DNAase, following manufacturer's instructions. The quality of the obtained RNA was assessed by an Agilent 2100 Bioanalyzer. Only high-quality RNA with RNA integrity numbers (RINs over 7.5) was used (13 for brain, 6 for liver and 4 for skeletal muscle; 1:1 ratio of torpor: active organisms). RNA quantity was estimated using the Kit Quant-iTTM RiboGreen® RNA in a DQ300 Hoefer fluorometer. Individual cDNA libraries (N=25) were labeled with sample-specific barcode adaptors, normalized and randomly built using the TrueSeq RNA Sample Preparation Kit v2 (Illumina; 0.5 µg of total RNA), following manufacturer's recommendations. These cDNA libraries were then pooled in equimolar ratios, with 2 or 3 randomly selected samples per pool, and were sequenced (2 × 150 bp PE) in eleven separated Illumina MiSeq runs at the AUSTRAL-*omics* Core Facility, Facultad de Ciencias, Universidad Austral de Chile (www.australomics.cl). Randomization of library preparation and sequencing is described as a way to avoid confounding experimental factors with technical factors (Conesa et al., 2016). Sequences were demultiplexed based on their sample-specific barcode adaptors.

193 Raw data from the sequencing runs were deposited at the Sequence Read Archive (SRA)
194 repository of the National Center for Biotechnology Information (NCBI) under accession
195 number SRR6255590- SRR6255614 of the Bioproject PRJNA416414. We eliminated
196 samples with RIN values below 7.0, which happened especially with skeletal muscle and
197 resulted in unbalanced final sample sizes among tissues.
198
199 *2.3 Bioinformatics*
200 Following sequencing, quality control (filtering and trimming) of the raw data was
201 performed using the Trimmomatic tool v.030 (Bolger, Lohse, & Usadel, 2014) and we
202 removed every read with a phred quality score of 30 or less, which gives 99.9% in base
203 accuracy. We used this phred score to be conservative and avoid multiple mappings, which
204 could produce isoforms as artifacts of incorrect mismatches (see a debate in Williams,
205 Baccarella, Parrish, & Kim, 2016). Still, some isoforms were produced which we interpret
206 according to the involved biological function. The quality trimmed reads were assembled
207 using Trinity 2.0.4 (Grabherr et al., 2011) with the standard Inchworm, Chrysalis and
208 Butterfly pipeline and a minimum contig length of 200 nt (De Wit et al., 2012). These
209 setting parameters have been optimized for de novo assemblies of non-model species with
210 Trinity (Grabherr et al., 2011). Duplicate sequences were then removed manually. The
211 quality and completeness of the assembly was analysed using the software QUAST for
212 assembly statistics (Gurevich, Saveliev, Vyahhi, & Tesler, 2013), and by mean of the
213 Benchmarking Universal Single-Copy Orthologs (BUSCO v.3) approach (Simao,
214 Waterhouse, Ioannidis, Kriventseva, & Zdobnov, 2015). For BUSCO, our analyses were
215 based on a subset of 233 (Core Vertebrate Genes, CVG) and 4104 (Mammalia) orthologs,

which in eukariotes are widely conserved core genes that generally lack paralogs (Simão et al., 2015).

Processed high quality reads were mapped to the assembled contigs using the Bowtie (version 2.0) read aligner (Langmead & Salzberg, 2012). To improve isoform counts, we used the RNA-Seq by Expectation Maximization (RSEM, version 1.0) software (Li & Dewey, 2011) that assesses transcript abundance in the assembled transcriptome. Then, a sample-based clustering analysis (heatmap of Euclidean distances) was performed in order to identify the distribution of the samples according to the experimental conditions using the R function *dist* and the function *heatmap.2* from the gplots package. Our de novo assembled transcriptome was blasted against the UniProt (Swiss-Prot and TrEMBL), KOBAS and NCBI RefSeq (nr) protein databases using the BLASTX algorithm with an e-value cutoff of $1e^{-5}$ (Altschul, Gish, Miller, Myers, & Lipman, 1990). With this procedure, the annotation was performed against a database containing several million proteins. Annotated unigenes (consensus, non-redundant sequences) were further searched for Gene Ontology (GO) terms using Blast2GO software (**www.blast2go.com**)(Conesa et al., 2005) according to the main categories of Gene Ontology (GO; molecular functions, biological processes and cellular components) (Ashburner et al., 2000). Complementary annotations were done with the InterProScan v.5 software (Jones et al., 2014), which provides functional analysis of proteins by classifying them into families and predicting domains and important sites. The annotation results were further fine-tuned with the Annex and GO slim functions of the Blast2GO software in order to improve and summarize the functional information of the transcriptome dataset. Additionally, proteins were finally annotated using the Kyoto Encyclopedia of Genes and Genomes (KEGG) and its automated assignment server (KAAS) (Moriya, Itoh, Okuda, Yoshizawa, & Kanehisa, 2007).

240

241 *2.4 Differential gene expression analysis*

242 Differentially expressed genes (DEGs), were identified using the R/Bioconductor
243 package DESeq2 v.1.10 (Love, Huber, & Anders, 2014) with raw read counts. The
244 estimated counts were normalized against the size of the transcriptome and the total number
245 of readings that were mapped per sample, using the regularized logarithm (rlog) method in
246 DESeq2 and expressed in a log2 scale. Basically, DESeq2 normalizes the counts by
247 dividing each column of the count table (samples) by the size factor of this column. The
248 size factor is then calculated by dividing the samples by the geometric means of the genes,
249 which brings the count values to a common scale suitable for comparison (Love et al.,
250 2014). P-values for differential expression were calculated using a negative binomial test
251 for differences between the base means of the control and torpor conditions. The P-values
252 were adjusted for multiple test correction using Ward's method with the Benjamini-
253 Hochberg procedure (Ferreira & Zwinderman, 2006). Significant DEGs were defined as
254 those genes with an adjusted p-value (false discovery rate, FDR) ≤ 0.05 and $\log_2$ (fold
255 change) ≥ 1. Differentially expressed genes across samples were visualized using standard
256 volcano plots, where $\log_2$ fold change was plotted against $\log_{10}$ (FDR adjusted p-value).
257 Furthermore, heatmaps were produced to visualize gene expression across samples and
258 tissues using z-scores (based on normalized counts) and plotted with the Heatmapper
259 software (Babicki et al., 2016).

260 Enrichment of GO and KEGG pathways in genes up- and down-regulated during
261 torpor were analyzed using Blast2GO (Fisher's exact test) and the goseq R package
262 (Young, Wakefield, Smyth, & Oshlack, 2010), with a threshold false discovery rate of
263 0.001. The reference used was the whole transcripts with GO slim annotation. Chord

264 diagrams to visualize enriched pathways were drawn using Circos (Krzywinski et al.,
265 2009).

266
267 **3. Results**

268 In this study, a total of 414 million of reads were generated from 23 libraries
269 derived from brain (13), liver (6) and skeletal muscle (4) of active and hibernating *D.*
270 *gliroides* (mean = 8.6 million of reads per sample; see Supplementary Table 1). After a
271 stringent filtering process, ~94% high-quality, adapter-free and non-redundant reads were
272 retained for further downstream analyses. Our *de novo* assembly generated 507,815
273 contiguous sequences (putative transcripts, contigs) with a mean sequence length of 718 bp,
274 an N50 of 1,387 bp and an L50 of 6,0430. The longest sequence contains 68,683 bp and
275 16% of the sequences were over 1k bp. The assessment of transcriptome completeness
276 using the Benchmarking Universal Single-Copy Orthologs (BUSCO) approach, identified a
277 high representation of Core Vertebrate Genes (CVG), with 94.4% marked as complete and
278 98.1% as complete + partial. Only 1.29% of the CVG were missing. Similarly, our BUSCO
279 analysis revealed 3,577 (87%) complete and 3,929 (95.74%) complete + partial
280 Mammalian Core Genes (MCG). From this reference gene set, 175 (4.26%) MCG were
281 missing in our *de novo* assembly. In terms of the functional association of the putative
282 transcripts in the *de novo* assembled transcriptome of *D. gliroides*, our analysis produced
283 31,438 contigs that were blasted to known proteins in the public databases NCBI (nr),
284 KOBAS and UniProt (Swiss-Prot and TrEMBL) were linked to GO classifications (average
285 4.55 GOs per contig). Hypothetical or predicted proteins in these databases were excluded
286 by discarding matches associated to “hypothetical”, “predicted”, “unknown” and “putative”
287 categories. Most of the annotated contigs (93%) hit against the koala (*Phascolarctos*

cinereus), the gray short-tailed opossum (*Monodelphis domestica*) and the Tasmanian devil (*Sarcophilus harrisii*) genomes, in this order.

Our transcriptomic survey of hibernating *D. gliroides* identified 73,125 mRNA transcripts in the brain, of which 594 exhibited differential regulation during torpor; 225 of them were down-regulated and 369 up-regulated (Fig 1A). Some of the very highly differentially expressed genes are named on the figure. In the liver, we identified 36,865 transcripts with 226 showing differential regulation during torpor: 79 down-regulated and 147 up-regulated (Fig 1B). In skeletal muscle, these numbers were 13,038 total transcripts with 85 differentially regulated during torpor: 35 down-regulated and 50 up-regulated (Fig 1C). We found 317 transcripts that were exclusively up-regulated in the brain, 131 transcripts that were exclusively up-regulated in the liver, and 44 transcripts exclusively up-regulated in muscle (Fig. 1D; upper panel). Oppositely, 191 transcripts were exclusively down-regulated in the brain, 73 in the liver and 46 in muscle (Fig. 1D; lower panel). A few transcripts were up-regulated or down-regulated in common among two or all three of the organs; these are named in Fig 1D and more details about their functions are given in Supplementary Tables 2 to 7. For example, *SETDB1, SCL25A18 and ACADVL* were up-regulated in both brain and liver whereas *EIF2AK1* was up-regulated in both brain and muscle. Only one transcript, encoding thioredoxin-interacting protein (*TXNIP*; Fig 1), was up-regulated in common in all three tissues and also fell within the top ten upregulated genes in each of these organs (see Supplementary Tables). This gene is described as encoding potent antioxidant protein associated with a number of human diseases (see Discussion).

Functions such as protection against reactive oxygen species (gene: *TXNIP*; overexpressed in all three organs of hibernators: Fig 1A-C; Fig 2A), inhibition of

transcription (genes: *HIST2H2A*; *SRSF5*; Fig 1A, Fig 2), fuel switch to fat metabolism (genes: *ZNF638, ATG3*; Fig 1D,F; Fig 2) and inhibition of angiogenesis (*ANGPTL4*; Fig 1C), appeared as the most important changes in the brain (Fig 1; Supplementary Tables 2 and 3). In the liver, the greatest changes in gene expression characterizing torpor seemed to be associated with the fuel switch from carbohydrate to lipid catabolism, since four genes involved in promoting fat catabolism enzymes were among the top five differentially expressed ones (*PDP2, CYB5R3*, overexpressed; *NR1H4, ND4,* under-expressed, Suppl. Table 4 and 5). In muscle, a similar interpretation indicated that mechanisms for avoiding muscle atrophy (over-expressed genes: *PVALB, EIF3D, GADPH*, Fig 4A-E; Supplementary Tables 4 and 5) may be the most important functions being exacerbated during torpor.

A functional enrichment analysis based on the gene-ontology database (GO) suggested that several metabolic pathways were enriched (both under-expressed and over-expressed) in the brain during torpor, compared with the other two organs, that only showed overexpression of a few biological functions (Fig 2A). This is also appreciated in the expression profiles of each organ (i.e., the "heatmaps", see Supplementary Fig 4). The analysis arising from the Kyoto Encyclopedia of Genes and Genomes (KEGG) showed a myriad of functions that were differentially regulated in the brain, such as cold sensitivity, circadian perception, mRNA surveillance, and stress response (Fig 2B). The liver and muscle profile, by contrast, indicated that the most important modified functions were orientated to the maintenance of organ function (e.g., biosynthesis of amino acids) and to fuel switch to lipid metabolism (e.g., fatty acid degradation, metabolic pathways) (Fig 2C, D).

4. Discussion

Today, comparative physiologists have a broad repertoire of technological tools that can be used to identify functional changes associated to a given physiological condition; from simple (and often inexpensive) measures of whole-animal metabolic fluxes (e.g., respirometry, blood biochemistry and haematology, tissue-specific enzymes and metabolites; see recent examples in Franco et al., 2013; Il'ina et al., 2017; Rouble & Storey, 2015) to the powerful characterization of exacerbated/enriched metabolic pathways that high throughput sequencing methods provide. To the best of our knowledge, this is the first RNA-seq analysis of hibernation in a marsupial, which provided a wealth of detailed information. In order to avoid being "lost in the map" (sensu Travisano & Shaw, 2013), we focus on some particularly important metabolic functions with relevance for torpor, provided by our de novo assembly. This procedure showed high completeness as evidenced for the percentage of coverage of Core Vertebrate Genes (CVG) and Mammalian Core Genes (MCG). The overall statistics of our assembly (N50, L50, contig length, number of contigs >1k), were similar to the results documented in *de novo* assembled transcriptomes of other mammals, such as the beaver (*Castor fiber L.*; testis; Bogacka et al., 2017), and the Nile grass rat (*Arvicanthis ansorgei*; retina; Liu et al., 2017). However, we had higher values compared with marsupials such as the long-nosed bandicoot (*Perameles nasuta*; heart, liver, spleen and kidney; Morris et al., 2018), and the Virginia opossum *Didelphis virginiana*; kidney; Eshbach et al., 2017).

4.1 Thioredoxin interacting protein and oxidative damage

The most notable finding of our analysis was the overexpression in all three organs of *TXNIP*, the gene encoding thioredoxin interacting protein. The TXNIP was first identified as an endogenous negative regulator of thioredoxin, a ubiquitous redox protein in cells that

is particularly involved in the reduction of oxidized cysteine residues and cleavage of disulfide bonds (Nishiyama et al., 1999). TXNIP has been linked, not just with an antioxidant/redox role (e.g. to minimize ischemia-reperfusion damage), but with the broader regulation of mitochondrial function to help suppress oxidative metabolism when oxygen is limiting, and shift metabolism to anaerobic glucose catabolism by mediating inhibition of pyruvate dehydrogenase (Chong et al., 2014; Spindel, World, & Berk, 2012; Yoshioka & Lee, 2014). Several diseases are associated with disruptions of the thioredoxin system, such as cataract formation, ischemic heart diseases, several cancers, diabetes complication and hypertension (Maulik & Das, 2008). TXNIP is also involved in inhibiting unnecessary glucose influx into cells while also promoting fatty acid oxidation (Hand et al., 2013); both of these are central features of a hibernating phenotype. Indeed, recent research has shown that the *TXNIP* gene was overexpressed in brain (hypothalamus), liver, and white and brown adipose during induced-torpor experiments in mice as well as in natural torpor in Siberian hamsters (*Phodopus sungorus*)(DeBalsi et al., 2014; Hand et al., 2013; Jastroch et al., 2016). Our current identification of a multi-organ strong upregulation of *TXNIP* in *D. gliroides* (including multiple gene variants in brain) adds further support for the proposal that TXNIP has a central role in the metabolic control of torpor.

4.2 Metabolic switch

In the brain, ANGPTL4 secretion (which we found strongly up-regulated) is of central importance in regulating the switch to a lipid-based fuel economy during torpor, facilitating lipid release from adipose and uptake by other tissues. Indeed, recent studies have reported significant upregulation of *ANGPTL4* transcripts in ground squirrel heart during torpor and interbout arousal stages of hibernation as compared with pre- or post-

hibernation months (Vermillion, Anderson, Hampton, & Andrews, 2015) as well as during torpor in a ground squirrel bone-marrow transcriptome when compared with summer animals (intermediate transcript levels were seen during interbout arousal) (Cooper et al., 2016). In the same vein, a powerful indicator of the suppression of carbohydrate fuel use within the brain during torpor is pyruvate dehydrogenase kinase 4 (*PDK4*), whose transcripts were strongly elevated in the brain. Phosphorylation of pyruvate dehydrogenase (PDH) at S232, S293 or S300 by any of four PDK isozymes inhibits its activity (Harris, Bowker-Kinley, Huang, & Wu, 2002) and is crucial for blocking the oxidation of pyruvate as a substrate, especially when carbohydrate reserves must be conserved. Indeed, strong suppression of PDH activity during hibernation has been widely reported in multiple tissues of eutherian hibernators (summarized in Wijenayake, Tessier, & Storey, 2017). Strong increases in PDH phosphorylation at 1, 2 or all 3 serine sites were also reported for six tissues (including brain, liver and skeletal muscle) of *D. gliroides* (Wijenayake et al., 2017) and the upregulation of *PDK4* in brain (predictably elevating PDK4 protein) would support PDH inhibition and presumably help to direct brain to make greater use of ketones as substrates during hibernation.

4.3 Marsupial nonshivering thermogenesis

Uniquely in marsupials, liver appears to be the main site of nonshivering thermogenesis since brown adipose tissue is not present (Jastroch, Wuertz, Kloas, & Klingenspor, 2005; R. W. Rose, West, Ye, McCormack, & Colquhoun, 1999) and, hence, modulation of multiple controls on lipid metabolism is probably needed to regulate this novel liver function (Hadj-Moussa et al., 2016). Among down-regulated genes we found in liver, three deserve particular mention for their potential roles in the hibernating marsupial:

ND4, NR1H4 and *TCAF2* (see Supplementary Table 5). Transcript levels of the mitochondria-encoded NADH dehydrogenase subunit 4 (*ND4*) gene were strongly reduced in *D. gliroides* liver during hibernation. By contrast, strong increases in ND4 expression were reported in brown adipose tissue of the bat, *Myotis lucifugus* during hibernation (Eddy, Morin, & Storey, 2006) and *ND2* transcripts (also mitochondria-encoded) were elevated during hibernation in heart and skeletal muscle of 13-lined ground squirrels, *Spermophilus tridecemlineatus* (Fahlman, Storey, & Storey, 2000). Compared with *D. gliroides,* this suggests that there may be either tissue-specific (liver versus muscle/BAT) or marsupial vs eutherian differences in the reorganization of mitochondrial oxidative metabolism in the torpid state. On the other hand, *NR1H4* encodes the NR1H4 protein (nuclear receptor subfamily 1, group H, member 4) that is also known as the bile acid receptor (BAR) or the farnesoid X receptor (FXR). This receptor is a master regulator of hepatic triglyceride, cholesterol and bile acid metabolism. Active FXR exerts controls that suppress *de novo* lipogenesis and promote FFA oxidation. FXR gene expression was also reduced in liver of hibernating ground squirrels compared with summer animals (Nelson, Otis, & Carey, 2009) and also occurs in non-alcoholic fatty liver disease in humans. FXR-deficient mice not only exhibited marked hepatosteatosis (fatty liver) and hypertriglyceridemia (Jiao, Lu, & Li, 2015; Wollam & Antebi, 2011) but showed an accelerated fasting-induced entry into torpor and markedly greater cold-intolerance as compared with controls (Cariou et al., 2007). Hence, the strong suppression of *NR1H4* transcript levels (implying suppressed FXR protein levels) in liver of hibernating *D. gliroides*, suggests a role for this receptor in the management and/or restructuring of liver lipid metabolism during hibernation when fatty acid oxidation is the primary mode of ATP production. This, together with previous results in *D. gliroides* and also in

Monodelphis domestica (Hadj-Moussa et al., 2016; Villarin et al., 2003) provides an intriguing role between FXR (BAR) function, lipid metabolism and NST in the liver metabolism of hibernating marsupials.

4.5 KEGG integrated analysis

The analysis based on the Kioto Encyclopedia of Genes and Genomes (KEGG, see Fig 2B) showed, in torpid animals, overexpression of multiple genes contributing to the mTOR signaling pathway (genes *SEH1L*, *SGK1*), circadian rhythm pathways (genes *CUL1*, *CRY2*), notch signaling pathway (genes *NCOR2*, *DTX3, EP300*), and ubiquitin-mediated proteolysis (genes *CUL1, UBE20, CDC34, UBA3, HUWE1*). Seh1 (known as SEH1L in mammals) is a subunit of the GATOR2 complex that is an essential activator of mTORC1 kinase. Seh1 is also a subunit of the Nup107 complex (the nucleoporin Y-complex) that plays a major role in formation of the nuclear pore complex in interphase and associates with kinetochores in mitosis (Platani, Samejima, Samejima, Kanemaki, & Earnshaw, 2018). SGK1, on the other hand, is one of many downstream targets of the mTOR C2 kinase, representing one arm of the mTORC2 signaling pathway (Garcia-Martinez & Alessi, 2008). Cry2 is one of the main circadian rhythm proteins, and it is known that this protein is upregulated during hibernation in hamsters and ground squirrels (Crawford et al., 2007).

The high level of transcriptional activity detected in the brain contrasts with the few enriched pathways of liver and muscle (Fig 2C and D). This, however, could be a consequence of the low sample size we had for those two organs (especially for muscle), which makes our conclusions regarding these organs, preliminary. Both for liver and

456 muscle we found a strong differential regulation (up- and down-regulation) of metabolic
457 pathways *sensu lato*, which is probably due to the physiological switch from carbohydrate
458 to lipid-based metabolism also described in other hibernators (Boyer & Barnes, 1999;
459 Storey & Storey, 2010; Villanueva-Canas et al., 2014), and in *D. gliroides* (Wijenayake et
460 al., 2018b). This is confirmed here, as we found strong overexpression of pathways related
461 to fatty acid degradation (genes *ACSL5, ACA*DVL) and regulation of autophagy (genes
462 *ULK1, ULK2, GABARAPL1*) in the liver (see Fig 2C). Hibernators all increase their content
463 of unsaturated FAs so that lipid depots can remain fluid at low Tb (Contreras, Franco,
464 Place, & Nespolo, 2014; J. C. Rose, Epperson, Carey, & Martin, 2011). Our findings
465 support this view, since differential up-regulation of ACSL5 (the protein acyl-CoA
466 synthetase long-chain 5) is used both in fatty acid synthesis and beta-oxidation. By contrast,
467 in muscle we found overexpression of the longevity-regulating pathway, which indicates
468 that differentially expressed genes in the muscle are directed toward the maintenance of
469 organ function, which in marsupials (in addition to the liver, as discussed before) is crucial
470 for rewarming (Hadj-Moussa et al., 2016; Opazo, Nespolo, & Bozinovic, 1999).
471
472 *5. Summary and conclusions*
473 In this paper, we have shown that the hibernating marsupial *D. gliroides* express
474 adaptive physiological mechanisms to deal with the consequences of hypometaboism and
475 cold during torpor. These mechanisms are tissue-specific and involve: (1) protection against
476 reactive oxygen species, ROS (i.e., oxidative damage) by overexpressing the *TXNIP* gene
477 among others, (2) metabolic switch from carbohydrate to fat-based metabolism in liver and
478 muscle, (3) nonshivering thermogenesis in the liver, (4) transcriptional suppression of non-
479 essential functions, (5) overexpression of proteins controlling circadian rhythm in the brain,

and (6) overexpression of longevity-regulated pathways that maintain organ function in muscle. In terms of survival and fitness, these physiological changes have the net consequence of making this metabolic depression, reversible and safe. Several of these mechanisms are conserved, previously described in placental mammals, but also described in *D. gliroides*. Some of them are apparently unique to marsupials (e.g., role of liver in rewarming), but still only described in a few species. Given that Microbiotherids are considered the ancestors of Australian marsupials (Mitchell et al., 2014), further studies in other marsupial species would be crucial to determine the generality of our findings.

Acknowledgements. This study was funded by Fondo Basal CAPES 0002-2014 to Francisco Bozinovic and MIISSB Iniciativa Científica Milenio (MIISSB). Juan Diego Gaitan acknowledges a CSIRO-OCE postdoctoral fellowship. Julian F. Quintero-Galvis acknowledges a Conicyt PhD fellowship N° 21160901. Roberto Nespolo acknowledges a Fondecyt grant N° 1180917. Andrea Silva acknowledges a Fondecyt grant N° 11140680. Kenneth B. Storey acknowledges NSERC Canada grant No 6793.

Author contributions

R.F.N designed the study, contributed to the experiment execution and wrote the manuscript. J.D.G-E contributed with the experiment design, contributed to the experiment execution, performed the final bioinformatic analysis and contributed with manuscript editions. J.F.Q-G collaborated with the experiment, contributed with data analysis and contributed with manuscript editions. F.V.F contributed with manuscript editions and data analysis. A.X.S contributed to the experiment execution and with the bioinformatic analysis. C.M performed the initial bioinformatic analysis and contributed with manuscript editions in the methods section. K.B.S contributed with manuscript editions and discussion regarding the hibernating phenotype. F.B funded the study, contributed with the experiment design and contributed with manuscript editions.

Data accessibility statement

The data presented in this paper will be accessible in dryad and raw data from the sequencing runs were deposited at the Sequence Read Archive (SRA) repository of the National Center for Biotechnology Information (NCBI) under accession number SRR6255590- SRR6255614 of the Bioproject PRJNA416414.

Competing interests statement

The authors declare no competing interests

Figure captions

Fig 1. A-C Volcano plots showing differentially regulated genes at the P=0.05 level (green, horizontal line) in three tissues of torpid *D. gliroides* as compared with active animals. Significantly down-regulated genes are indicated as negative fold change (blue), and up-regulated genes are indicated as positive values (red). The gray zone indicates the number of transcripts that do not show significant differential expression. A: brain; B: liver; C: skeletal muscle. D: commonly up-regulated genes among organs (upper panel) and commonly down-regulated genes (bottom panel). The numbers represent the numbers of transcripts that were differentially regulated exclusively for each organ (e.g., 44 transcripts were exclusively and significantly up-regulated in muscle). Most differentially regulated genes are written in yellow and white font on the diagrams. Descriptions of the top 10 significantly regulated genes are provided in Supplementary Tables 2 to 7). Several isoforms of the *TXNIP* gene were found among the upregulated genes in brain, which are denoted by the red ellipse (Fig 1A).

Fig 2. Functional enrichment analysis of genes that appeared over-represented during torpor using the gene ontology database (A). The size of the circles represents the number of differentially expressed genes over the total number of genes, associated to a given GO term; whereas the color indicates the level of significance. Also a functional enrichment analysis using the Kyoto Encyclopedia of Genes and Genomes (KEGG-database) is shown for brain (B), liver (C) and muscle (D). In this analysis, genes are indicated at the left side of each pie graph, with the respective level of expression (Log2 FC) indicated in color in the small squares, and metabolic pathways are indicated in the right side of the graph, connected to the group of genes that are associated to the pathway by lines.

Supplementary Fig 1. Top five overexpressed (top panel) and under-expressed (bottom panel) genes found in the brain of torpid (n=7) and active (n=6) monito del monte expressed in transcripts per million sequences (TPM, mean ± SEM). Gene names and $\log_2$[fold-change] (FC) values are as follows: (A) *TXNIP* = thioredoxin-interacting protein (FC=2.43); (B) *HIST2H2AC* = histone H2A type 2C (FC =2.10); (C) *ANGPTL4* = angiopoietin-related protein 4 (FC = 1.88); (D) *ZNF638* = zinc finger protein 638 (FC = 1.76); (E) *GPR34* = G-protein coupled receptor 34(FC = 1.67); (F) *ATG3* = ubiquitin like-conjugating enzyme ($\log_2$ fold-change= -1.54); (G) *SRSF5* = serine/arginine-rich splicing factor 5 (FC = -1.33); (H) *SF3A1* = splicing factor 3A subunit 1 (FC = -1.30); (I) *TMED3* = transmembrane emp24 domain containing protein 3 (FC = -1.27); (J) *KCNJ13* = inward rectifier potassium channel 13 (FC = -1.24). Fold-change represents the times a transcript was found over-expressed or under-expressed relative to the active control (i.e., a $\log_2$ fold change = 2.85 means $2^{2.85}$ times overexpression; negative fold-changes mean under-expression). More details about these genes and the functions of the proteins that they encode are given in Supplementary Tables 2 to 7.

Supplementary Fig 2. Top five overexpressed (top panel) and under-expressed (bottom panel) genes found in the liver of torpid (n=3) and active (n=3) individuals expressed in transcripts per million sequences (TPM, mean ± SEM). Gene names and $\log_2$[fold-change]

(FC) values are as follows: (A) *GARS* = glycine-tRNA ligase (FC=6.82); (B) *PER3* = period circadian protein homolog 3 (FC =6.46); (C) *PDP2* = pyruvate dehydrogenase phosphatase (mitochondrial) (FC = 6.10); (D) *CYB5R3* = NADH- cytochrome b5 reductase 3 isoform X1 (FC = 6.09); (E) *TXNIP* = thioredoxin-interacting protein (FC=6.03); (F) *TCAF2* = TRPM8 channel-associated factor 2 isoform X2 (FC = -5.97); (G) *NR1H4* = nuclear receptor subfamily 1, group H, member 4 also known as the bile acid receptor (BAR) or the farnesoid X receptor (FXR) (FC = -5.81); (H) *KLHDC3* = kelch domain-containing protein 3 (FC = -5.53); (I) *ND4* = NADH dehydrogenase subunit 4 (mitochondrial) (FC = -5.49); (J) *SLC2A9* = Solute carrier family 2, facilitated glucose transporter member 9 (FC = -5.41). More details about these genes and the functions of the proteins that they encode are given in Supplementary Tables 2 to 7. Some bars are at zero because no transcripts were detected for such gene and condition.

Supplementary Fig 3. Top five overexpressed (top panel) and under-expressed (bottom panel) genes found in skeletal muscle or torpid (n=2) and active (n=2) individuals expressed in transcripts per million sequences (TPM, mean ± SEM). Gene names and $\log_2$[fold-change] (FC) values are as follows: (A) *PVALB* = parvalbumin alpha (FC=7.99); (B) *TXNIP* = thioredoxin-interacting protein (FC=6.09); (C) *DDX17* = ATP-dependent RNA helicase (FC=5.79); (D) *EIF3D* = eukaryotic translation initiation factor 3 subunit D (FC=5.76); (E) *GAPDH* = glyceraldehyde-3-phosphate dehydrogenase (FC=5.65); (F) *ABCB8* = ATP binding cassette subfamily B (mitochondrial)(FC=-5.33); (G) *DDI2* = protein DDI1 homolog 2 (FC=-5.07); (H) *SBF2* = myotubularin-related protein 2 (FC = -4.58); (I) *STXBP2* = syntaxin-binding protein 2 (FC = -4.51); (j) *CEP85* = centrosomal protein of 85 kDa (FC = -4.43). More details about these genes and the functions of the proteins that they encode are given in Supplementary Tables 2 to 7. Some bars at zero because no transcripts were detected for such gene and condition.

Supplementary Fig 4. Expression profiles of each organ, per individual, per treatment ("heatmaps"). Each individual and condition (e.g., Torpor1, Torpor2, Active1, Active2, etc), is indicated at the X-axis. The expression level [an adimensional Z-score based on log(FC)] is indicated by the color (under-expressed genes in blue; overexpressed genes in red). Each gene is indicated as a list, at the right side of each profile (only significantly regulated genes are shown, according to the log(FDR) adjusted values of Fig 1A-C). Lines at the left side of each profile indicate gene clustering according to their expression patterns.

References

Altschul, S. F., Gish, W., Miller, W., Myers, E. W., & Lipman, D. J. (1990). BASIC LOCAL ALIGNMENT SEARCH TOOL. *Journal of molecular biology, 215*(3), 403-410. doi:10.1006/jmbi.1990.9999

Andres-Mateos, E., Mejias, R., Soleimani, A., Lin, B. M., Burks, T. N., Marx, R., . . . Cohn, R. D. (2012). Impaired skeletal muscle regeneration in the absence of fibrosis during hibernation in 13-lined ground squirrels. *Plos One, 7*(11), e48884. doi:e48884 10.1371/journal.pone.0048884

610 Andrews, M. T. (2004). Genes controlling the metabolic switch in hibernating
611 mammals. *Biochemical Society Transactions, 32*, 1021-1024.
612 Ashburner, M., Ball, C. A., Blake, J. A., Botstein, D., Butler, H., Cherry, J. M., . . . Gene
613 Ontology, C. (2000). Gene Ontology: tool for the unification of biology. *Nature*
614 *Genetics, 25*(1), 25-29.
615 Babicki, S., Arndt, D., Marcu, A., Liang, Y. J., Grant, J. R., Maciejewski, A., & Wishart, D. S.
616 (2016). Heatmapper: web-enabled heat mapping for all. *Nucleic Acids Research,*
617 *44*(W1), W147-W153. doi:10.1093/nar/gkw419
618 Bogacka, I., Paukszto, T., Jastrzebski, J. P., Czerwinska, J., Chojnowska, K., Kaminska, B.,
619 . . . Kaminski, T. (2017). Seasonal differences in the testicular transcriptome
620 profile of free-living European beavers (Castor fiber L.) determined by the
621 RNA-Seq method. *Plos One, 12*(7), 20. doi:10.1371/journal.pone.0180323
622 Bolger, A. M., Lohse, M., & Usadel, B. (2014). Trimmomatic: a flexible trimmer for
623 Illumina sequence data. *Bioinformatics, 30*(15), 2114-2120.
624 doi:10.1093/bioinformatics/btu170
625 Boyer, B. B., & Barnes, B. M. (1999). Molecular and metabolic aspects of mammalian
626 hibernation. *Bioscience, 49*, 713-724.
627 Boyles, J. G., Thompson, A. B., McKechnie, A. E., Malan, E., Humphries, M. M., & Careau,
628 V. (2013). A global heterothermic continuum in mammals. *Global Ecology and*
629 *Biogeography, 22*(9), 1029-1039. doi:10.1111/geb.12077
630 Bozinovic, F., Ruiz, G., & Rosenmann, M. (2004). Energetics and torpor of a South
631 American "living fossil", the Microbiotheriid *Dromiciops gliroides*. *Journal of*
632 *Comparative Physiology B, 174*, 293-297.
633 Carey, H. V., Andrews, M. T., & Martin, S. L. (2003). Mammalian hibernation: Cellular
634 and molecular responses to depressed metabolism and low temperature.
635 *Physiological Reviews, 83*(4), 1153-1181. doi:10.1152/physrev.00008.2003
636 Cariou, B., Bouchaert, E., Abdelkarim, M., Dumont, J., Caron, S., Fruchart, J. C., . . . Staels,
637 B. (2007). FXR-deficiency confers increased susceptibility to torpor. *FEBS*
638 *letters, 581*(27), 5191-5198. doi:10.1016/j.febslet.2007.09.064
639 Chong, C. R., Chan, W. P. A., Nguyen, T. H., Liu, S. F., Procter, N. E. K., Ngo, D. T., . . .
640 Horowitz, J. D. (2014). Thioredoxin-Interacting Protein: Pathophysiology and
641 Emerging Pharmacotherapeutics in Cardiovascular Disease and Diabetes.
642 *Cardiovascular Drugs and Therapy, 28*(4), 347-360. doi:10.1007/s10557-014-
643 6538-5
644 Conesa, A., Gotz, S., Garcia-Gomez, J. M., Terol, J., Talon, M., & Robles, M. (2005).
645 Blast2GO: a universal tool for annotation, visualization and analysis in
646 functional genomics research. *Bioinformatics, 21*(18), 3674-3676.
647 doi:10.1093/bioinformatics/bti610
648 Contreras, C., Franco, M., Place, N. J., & Nespolo, R. F. (2014). The effects of poly-
649 unsaturated fatty acids on the physiology of hibernation in a South American
650 marsupial, Dromiciops gliroides. *Comparative Biochemistry and Physiology a-*
651 *Molecular & Integrative Physiology, 177*, 62-69. doi:10.1016/j.cbpa.2014.07.004
652 Cooper, S. T., Sell, S. S., Fahrenkrog, M., Wilkinson, K., Howard, D. R., Bergen, H., . . .
653 Hampton, M. (2016). Effects of hibernation on bone marrow transcriptome in
654 thirteen-lined ground squirrels. *Physiological Genomics, 48*(7), 513-525.
655 doi:10.1152/physiolgenomics.00120.2015

Crawford, F. I. J., Hodgkinson, C. L., Ivanova, E., Logunova, L. B., Evans, G. J., Steinlechner, S., & Loudon, A. S. I. (2007). Influence of torpor on cardiac expression of genes involved in the circadian clock and protein turnover in the Siberian hamster (Phodopus sungorus). *Physiological Genomics, 31*(3), 521-530. doi:10.1152/physiolgenomics.00131.2007

De Wit, P., Pespeni, M. H., Ladner, J. T., Barshis, D. J., Seneca, F., Jaris, H., . . . Palumbi, S. R. (2012). The simple fool's guide to population genomics via RNA-Seq: an introduction to high-throughput sequencing data analysis. *Molecular Ecology Resources, 12*(6), 1058-1067. doi:10.1111/1755-0998.12003

DeBalsi, K. L., Wong, K. E., Koves, T. R., Slentz, D. H., Seiler, S. E., Wittmann, A. H., . . . Lark, D. S. (2014). Targeted metabolomics connects thioredoxin-interacting protein (TXNIP) to mitochondrial fuel selection and regulation of specific oxidoreductase enzymes in skeletal muscle. *Journal of Biological Chemistry, 289*(12), 8106-8120.

Eddy, S. F., Morin, P. J. R., & Storey, K. B. (2006). Differential expression of selected mitochondrial genes in hibernating little brown bats, Myotis lucifiugus. *Journal of Experimental Zoology Part a-Comparative Experimental Biology, 305A*(8), 620-630. doi:10.1002/jez.a.294

Eshbach, M. L., Sethi, R., Avula, R., Lamb, J., Hollingshead, D. J., Finegold, D. N., . . . Weisz, O. A. (2017). The transcriptome of the Didelphis virginiana opossum kidney OK proximal tubule cell line. *American Journal of Physiology-Renal Physiology, 313*(3), F585-F595. doi:10.1152/ajprenal.00228.2017

Faherty, S. L., Villanueva-Canas, J. L., Klopfer, P. H., Alba, M. M., & Yoder, A. D. (2016). Gene Expression Profiling in the Hibernating Primate, Cheirogaleus Medius. *Genome Biology and Evolution, 8*(8), 2413-2426. doi:10.1093/gbe/evw163

Fahlman, A., Storey, J. M., & Storey, K. B. (2000). Gene up-regulation in heart during mammalian hibernation. *Cryobiology, 40*(4), 332-342. doi:10.1006/cryo.2000.2254

Fedorov, V. B., Goropashnaya, A. V., Stewart, N. C., Toien, O., Chang, C., Wang, H. F., . . . Barnes, B. M. (2014). Comparative functional genomics of adaptation to muscular disuse in hibernating mammals. *Molecular Ecology, 23*(22), 5524-5537. doi:10.1111/mec.12963

Ferreira, J. A., & Zwinderman, A. H. (2006). On the Benjamini-Hochberg method. *Annals of Statistics, 34*(4), 1827-1849. doi:10.1214/009053606000000425

Fons, R., Sender, S., Peters, T., & Jurgens, K. D. (1997). Rates of rewarming, heart andrespiratory rates and their significance for oxygen transport during arousal from torpor in the smallest mammal, the etruscan shrew *Suncus etruscus*. *Journal of Experimental Biology, 200*, 1451-1458.

Franco, M., Contreras, C., & Nespolo, R. F. (2013). Profound changes in blood parameters during torpor in a South American marsupial. *Comparative Biochemistry and Physiology a-Molecular & Integrative Physiology, 166*(2), 338-342. doi:10.1016/j.cbpa.2013.07.010

Franco, M., Contreras, C., Place, N. J., Bozinovic, F., & Nespolo, R. F. (2017). Leptin levels, seasonality and thermal acclimation in the Microbiotherid marsupial Dromiciops gliroides: Does photoperiod play a role? *Comparative Biochemistry*

and Physiology a-Molecular & Integrative Physiology, 203, 233-240. doi:10.1016/j.cbpa.2016.09.025

Gannon, W. L., Sikes, R. S., & Comm, A. C. U. (2007). Guidelines of the American Society of Mammalogists for the use of wild mammals in research. *Journal of Mammalogy, 88*(3), 809-823. doi:10.1644/06-mamm-f-185r1.1

Garcia-Martinez, J. M., & Alessi, D. R. (2008). mTOR complex 2 (mTORC2) controls hydrophobic motif phosphorylation and activation of serum- and glucocorticoid-induced protein kinase 1 (SGK1). *Biochemical Journal, 416*, 375-385. doi:10.1042/bj20081668

Geiser, F., & Martin, G. M. (2013). Torpor in the Patagonian opossum (Lestodelphys halli): implications for the evolution of daily torpor and hibernation. *Naturwissenschaften, 100*(10), 975-981. doi:10.1007/s00114-013-1098-2

Grabherr, M. G., Haas, B. J., Yassour, M., Levin, J. Z., Thompson, D. A., Amit, I., . . . Regev, A. (2011). Full-length transcriptome assembly from RNA-Seq data without a reference genome. *Nature Biotechnology, 29*(7), 644-U130. doi:10.1038/nbt.1883

Graves, J. A. M., & Renfree, M. B. (2013). Marsupials in the Age of Genomics. In A. Chakravarti & E. Green (Eds.), *Annual Review of Genomics and Human Genetics, Vol 14* (Vol. 14, pp. 393-420). Palo Alto: Annual Reviews.

Gurevich, A., Saveliev, V., Vyahhi, N., & Tesler, G. (2013). QUAST: quality assessment tool for genome assemblies. *Bioinformatics, 29*(8), 1072-1075. doi:10.1093/bioinformatics/btt086

Habel, J. C., Assman, T., Schmidtt, T., & Avise, J. C. (2010). Relict species: from past to future. In J. C. Habel & T. Assman (Eds.), *Relict Species. Phylogeography and Conservation Biology*. Berlin: Springer.

Hadj-Moussa, H., Moggridge, J. A., Luu, B. E., Quiuntero-Galvis, J. F., Gaitan-Espitia, J. D., Nespolo, R. F., & Storey, K. B. (2016). The hibernating South American marsupial, Dromiciops gliroides, display torpor-sensititve microRNA expression patterns. *Scientific Reports*. doi:DOI: 10.1038/srep24627

Hand, L. E., Saer, B. R. C., Hui, S. T., Jinnah, H. A., Steinlechner, S., Loudon, A. S. I., & Bechtold, D. A. (2013). Induction of the Metabolic Regulator Txnip in Fasting-Induced and Natural Torpor. *Endocrinology, 154*(6), 2081-2091. doi:10.1210/en.2012-2051

Harris, R. A., Bowker-Kinley, M. M., Huang, B. L., & Wu, P. F. (2002). Regulation of the activity of the pyruvate dehydrogenase complex. In G. Weber (Ed.), *Advances in Enzyme Regulation, Vol 42, Proceedings* (Vol. 42, pp. 249-259). Oxford: Pergamon-Elsevier Science Ltd.

Hershkovitz, P. (1999). Dromiciops gliroides Thomas, 1894, Last of the Microbiotheria (Marsupialia), with a review of the family Microbiotheridae. *Fieldana, 93*, 1-60.

Hindle, A. G., Karimpour-Fard, A., Epperson, L. E., Hunter, L. E., & Martin, S. L. (2011). Skeletal muscle proteomics: carbohydrate metabolism oscillates with seasonal and torpor-arousal physiology of hibernation. *American Journal of Physiology-Regulatory Integrative and Comparative Physiology, 301*(5), R1440-R1452. doi:10.1152/ajpregu.00298.2011

Il'ina, T. N., Ilyukha, V. A., Baishnikova, I. V., Belkin, V. V., Sergina, S. N., & Antonova, E. P. (2017). Antioxidant defense system in tissues of semiaquatic mammals.

Journal of Evolutionary Biochemistry and Physiology, 53(4), 282-288. doi:10.1134/s0022093017040044

Jastroch, M., Giroud, S., Barrett, P., Geiser, F., Heldmaier, G., & Herwig, A. (2016). Seasonal Control of Mammalian Energy Balance: Recent Advances in the Understanding of Daily Torpor and Hibernation. *Journal of Neuroendocrinology, 28*(11), 10. doi:10.1111/jne.12437

Jastroch, M., Wuertz, S., Kloas, W., & Klingenspor, M. (2005). Uncoupling protein 1 in fish uncovers an ancient evolutionary history of mammalian nonshivering thermogenesis. *Physiological Genomics, 22*(2), 150-156. doi:10.1152/physiolgenomics.00070.2005

Jiao, Y., Lu, Y., & Li, X. Y. (2015). Farnesoid X receptor: a master regulator of hepatic triglyceride and glucose homeostasis. *Acta Pharmacologica Sinica, 36*(1), 44-50. doi:10.1038/aps.2014.116

Jones, P., Binns, D., Chang, H. Y., Fraser, M., Li, W. Z., McAnulla, C., . . . Hunter, S. (2014). InterProScan 5: genome-scale protein function classification. *Bioinformatics, 30*(9), 1236-1240. doi:10.1093/bioinformatics/btu031

Koteja, P. (2004). The evolution of concepts on the evolution of endothermy in birds and mammals. *Physiological and Biochemical Zoology, 77*, 1043-1050.

Krzywinski, M., Schein, J., Birol, I., Connors, J., Gascoyne, R., Horsman, D., . . . Marra, M. A. (2009). Circos: An information aesthetic for comparative genomics. *Genome Research, 19*(9), 1639-1645. doi:10.1101/gr.092759.109

Langmead, B., & Salzberg, S. L. (2012). Fast gapped-read alignment with Bowtie 2. *Nature Methods, 9*(4), 357-U354. doi:10.1038/nmeth.1923

Li, B., & Dewey, C. N. (2011). RSEM: accurate transcript quantification from RNA-Seq data with or without a reference genome. *Bmc Bioinformatics, 12*, 16. doi:10.1186/1471-2105-12-323

Liu, M. M., Farkas, M., Spinnhirny, P., Pevet, P., Pierce, E., Hicks, D., & Zack, D. J. (2017). De novo assembly and annotation of the retinal transcriptome for the Nile grass rat (Arvicanthis ansorgei). *Plos One, 12*(7), 14. doi:10.1371/journal.pone.0179061

Love, M. I., Huber, W., & Anders, S. (2014). Moderated estimation of fold change and dispersion for RNA-seq data with DESeq2. *Genome Biology, 15*(12), 38. doi:10.1186/s13059-014-0550-8

Luu, B. E., Wijenayake, S., Zhang, J., Tessier, S. N., Quintero-Galvis, J. F., Gaitan-Espitia, J. D., . . . Storey, J. M. (2018a). Strategies of biochemical adaptation for hibernation in a south American marsupial, Dromiciops gliroides: 2. Control of the Akt pathway and protein translation machinery. *Comparative Biochemical Physiology B*.

Luu, B. E., Wijenayake, S., Zhang, J., Tessier, S. N., Quintero-Galvis, J. F., Gaitan-Espitia, J. D., . . . Storey, K. B. (2018b). Strategies of biochemical adaptation for hibernation in a south American marsupial, Dromiciops gliroides: 3. Activation of pro-survival response pathways. *Comparative Biochemical Physiology B*.

Malan, A. (2010). Is the Torpor-Arousal Cycle of Hibernation Controlled by a Non-Temperature-Compensated Circadian Clock? *Journal of Biological Rhythms, 25*(3), 166-175. doi:10.1177/0748730410368621

Maulik, N., & Das, D. K. (2008). Emerging potential of thioredoxin and thioredoxin interacting proteins in various disease conditions. *Biochimica Et Biophysica Acta-General Subjects, 1780*(11), 1368-1382. doi:10.1016/j.bbagen.2007.12.008

Mitchell, K. J., Pratt, R. C., Watson, L. N., Gibb, G. C., Llamas, B., Kasper, M., . . . Cooper, A. (2014). Molecular Phylogeny, Biogeography, and Habitat Preference Evolution of Marsupials. *Molecular Biology and Evolution, 31*(9), 2322-2330. doi:10.1093/molbev/msu176

Morin, P., & Storey, K. B. (2009). Mammalian hibernation: differential gene expression and novel application of epigenetic controls. *International Journal of Developmental Biology, 53*(2-3), 433-442. doi:10.1387/ijdb.082643pm

Moriya, Y., Itoh, M., Okuda, S., Yoshizawa, A. C., & Kanehisa, M. (2007). KAAS: an automatic genome annotation and pathway reconstruction server. *Nucleic Acids Research, 35*, W182-W185. doi:10.1093/nar/gkm321

Morris, K. M., Weaver, H. J., O'Meally, D., Desclozeaux, M., Gillett, A., & Polkinghorne, A. (2018). Transcriptome sequencing of the long-nosed bandicoot (Perameles nasuta) reveals conservation and innovation of immune genes in the marsupial order Peramelemorphia. *Immunogenetics, 70*(5), 327-336. doi:10.1007/s00251-017-1043-1

Nelson, C. J., Otis, J. P., & Carey, H. V. (2009). A role for nuclear receptors in mammalian hibernation. *Journal of Physiology-London, 587*(9), 1863-1870. doi:10.1113/jphysiol.2008.167692

Nespolo, R. F., Bacigalupe, L. D., Figueroa, C. C., Koteja, P., & Opazo, J. C. (2011). Using new tools to solve an old problem: the evolution of endothermy in vertebrates. *Trends in Ecology & Evolution, 26*(8), 414-423. doi:10.1016/j.tree.2011.04.004

Nespolo, R. F., Verdugo, C., Cortes, P. A., & Bacigalupe, L. D. (2010). Bioenergetics of torpor in the Microbiotherid marsupial, Monito del Monte (*Dromiciops gliroides*): the role of temperature and food availability. *Journal of Comparative Physiology B-Biochemical Systemic and Environmental Physiology, 180*(5), 767-773. doi:10.1007/s00360-010-0449-y

Nishiyama, A., Matsui, M., Iwata, S., Hirota, K., Masutani, H., Nakamura, H., . . . Yodoi, J. (1999). Identification of thioredoxin-binding protein-2/vitamin D-3 up-regulated protein 1 as a negative regulator of thioredoxin function and expression. *Journal of Biological Chemistry, 274*(31), 21645-21650. doi:10.1074/jbc.274.31.21645

Opazo, J. C., Nespolo, R. F., & Bozinovic, F. (1999). Arousal from torpor in the chilean mouse-opposum (*Thylamys elegans*): does non-shivering thermogenesis play a role? *Comparative Biochemistry and Physiology A, 123*, 393-397.

Palma, R. E., & Spotorno, A. E. (1999). Molecular systematics of marsupials based on the rRNA 12S mitochondrial gene: The phylogeny of didelphimorphia and of the living fossil microbiotheriid Dromiciops gliroides Thomas. *Molecular Phylogenetics and Evolution, 13*(3), 525-535. doi:10.1006/mpev.1999.0678

Platani, M., Samejima, I., Samejima, K., Kanemaki, M. T., & Earnshaw, W. C. (2018). Seh1 targets GATOR2 and Nup153 to mitotic chromosomes. *Journal of Cell Science, 131*. doi:10.1242/jcs.213140

Renfree, M. B. (1981). Marsupials: alternative mammals. *Nature, 293*, 100-101.

838 Rose, J. C., Epperson, L. E., Carey, H. V., & Martin, S. L. (2011). Seasonal liver protein
839 differences in a hibernator revealed by quantitative proteomics using whole
840 animal isotopic labeling. *Comparative Biochemistry and Physiology D-Genomics*
841 *& Proteomics, 6*(2), 163-170. doi:10.1016/j.cbd.2011.02.003
842 Rose, R. W., West, A. K., Ye, J. M., McCormack, G. H., & Colquhoun, E. Q. (1999).
843 Nonshivering thermogenesis in a marsupial (the Tasmanian bettong Bettongia
844 gaimardi) is not attributable to brown adipose tissue. *Physiological and*
845 *Biochemical Zoology, 72*(6), 699-704. doi:10.1086/316709
846 Rouble, A. N., & Storey, K. B. (2015). Characterization of the SIRT family of NAW-
847 dependent protein deacetylases in the context of a mammalian model of
848 hibernation, the thirteen-lined ground squirrel. *Cryobiology, 71*(2), 334-343.
849 doi:10.1016/j.cryobiol.2015.08.009
850 Rouble, A. N., Tessier, S. N., & Storey, K. B. (2014). Characterization of adipocyte stress
851 response pathways during hibernation in thirteen-lined ground squirrels.
852 *Molecular and Cellular Biochemistry, 393*(1-2), 271-282. doi:10.1007/s11010-
853 014-2070-y
854 Ruf, T., & Geiser, F. (2015). Daily torpor and hibernation in birds and mammals.
855 *Biological Reviews, 90*(3), 891-926. doi:10.1111/brv.12137
856 Schwartz, C., Hampton, M., & Andrews, M. T. (2013). Seasonal and Regional
857 Differences in Gene Expression in the Brain of a Hibernating Mammal. *Plos One,*
858 *8*(3). doi:e58427
859 10.1371/journal.pone.0058427
860 Simao, F. A., Waterhouse, R. M., Ioannidis, P., Kriventseva, E. V., & Zdobnov, E. M.
861 (2015). BUSCO: assessing genome assembly and annotation completeness with
862 single-copy orthologs. *Bioinformatics, 31*(19), 3210-3212.
863 doi:10.1093/bioinformatics/btv351
864 Spindel, O. N., World, C., & Berk, B. C. (2012). Thioredoxin Interacting Protein: Redox
865 Dependent and Independent Regulatory Mechanisms. *Antioxidants & Redox*
866 *Signaling, 16*(6), 587-596. doi:10.1089/ars.2011.4137
867 Storey, K. B., & Storey, J. M. (2010). METABOLIC RATE DEPRESSION: THE
868 BIOCHEMISTRY OF MAMMALIAN HIBERNATION. In G. S. Makowski (Ed.),
869 *Advances on Clinical Chemistry, Vol 52* (Vol. 52, pp. 77-108).
870 Travisano, M., & Shaw, R. G. (2013). LOST IN THE MAP. *Evolution, 67*(2), 305-314.
871 doi:10.1111/j.1558-5646.2012.01802.x
872 Turner, J. M., Warnecke, L., Kortner, G., & Geiser, F. (2012). Opportunistic hibernation
873 by a free-ranging marsupial. *Journal of Zoology, 286*(4), 277-284.
874 doi:10.1111/j.1469-7998.2011.00877.x
875 van Breukelen, F., Krumschnabel, G., & Podrabsky, J. E. (2010). Vertebrate cell death in
876 energy-limited conditions and how to avoid it: what we might learn from
877 mammalian hibernators and other stress-tolerant vertebrates. *Apoptosis, 15*(3),
878 386-399. doi:10.1007/s10495-010-0467-y
879 van Breukelen, F., & Martin, S. L. (2015). The Hibernation Continuum: Physiological
880 and Molecular Aspects of Metabolic Plasticity in Mammals. *Physiology, 30*(4),
881 273-281. doi:10.1152/physiol.00010.2015
882 Vermillion, K. L., Anderson, K. J., Hampton, M., & Andrews, M. T. (2015). Gene
883 expression changes controlling distinct adaptations in the heart and skeletal

muscle of a hibernating mammal. *Physiological Genomics, 47*(3), 58-74. doi:10.1152/physiolgenomics.00108.2014

Villanueva-Canas, J. L., Faherty, S. L., Yoder, A. D., & Alba, M. M. (2014). Comparative Genomics of Mammalian Hibernators Using Gene Networks. *Integrative and Comparative Biology, 54*(3), 452-462. doi:10.1093/icb/icu048

Villarin, J. J., Schaeffer, P. J., Markle, R. A., & Lindstedt, S. L. (2003). Chronic cold exposure increases liver oxidative capacity in the marsupial Monodelphis domestica *Comparative Biochemistry and Physiology a-Molecular & Integrative Physiology, 136*(3), 621-630.

Wijenayake, S., Luu, B. E., Zhang, J., Tessier, S. N., Quintero-Galvis, J. F., Gaitan-Espitia, J. D., . . . Storey, K. B. (2018a). Strategies of biochemical adaptation for hibernation in a south American marsupial Dromiciops gliroides: 1. Mitogen-activated protein kinases and the cell stress response. *Comparative Biochemical Physiology B*.

Wijenayake, S., Luu, B. E., Zhang, J., Tessier, S. N., Quintero-Galvis, J. F., Gaitan-Espitia, J. D., . . . Storey, K. B. (2018b). Strategies of biochemical adaptation for hibernation in a South American marsupial, Dromiciops gliroides: 4. Regulation of pyruvate dehydrogenase complex and metabolic fuel selection. *Comparative Biochemical Physiology B*.

Wijenayake, S., Tessier, S. N., & Storey, K. B. (2017). Regulation of pyruvate dehydrogenase (PDH) in the hibernating ground squirrel, (Ictidomys tridecemlineatus). *Journal of Thermal Biology, 69*, 199-205. doi:10.1016/j.jtherbio.2017.07.010

Williams, C. R., Baccarella, A., Parrish, J. Z., & Kim, C. C. (2016). Trimming of sequence reads alters RNA-Seq gene expression estimates. *Bmc Bioinformatics, 17*, 13. doi:10.1186/s12859-016-0956-2

Wollam, J., & Antebi, A. (2011). Sterol Regulation of Metabolism, Homeostasis, and Development. In R. D. Kornberg, C. R. H. Raetz, J. E. Rothman, & J. W. Thorner (Eds.), *Annual Review of Biochemistry, Vol 80* (Vol. 80, pp. 885-916). Palo Alto: Annual Reviews.

Yoshioka, J., & Lee, R. T. (2014). Thioredoxin-interacting protein and myocardial mitochondrial function in ischemia-reperfusion injury. *Trends in Cardiovascular Medicine, 24*(2), 75-80. doi:10.1016/j.tcm.2013.06.007

Young, M. D., Wakefield, M. J., Smyth, G. K., & Oshlack, A. (2010). Gene ontology analysis for RNA-seq: accounting for selection bias. *Genome Biology, 11*(2), 12. doi:10.1186/gb-2010-11-2-r14

Zietak, M., Chabowska-Kita, A., & Kozak, L. P. (2017). Brown fat thermogenesis: Stability of developmental programming and transient effects of temperature and gut microbiota in adults. *Biochimie, 134*, 93-98. doi:10.1016/j.biochi.2016.12.006

A functional transcriptomics analysis in the relict marsupial *Dromiciops gliroides* reveals adaptive regulation of protective functions during hibernation

Roberto F. Nespolo[1,2,3], Juan Diego Gaitan-Espitia[4,5], Julian F. Quintero-Galvis[1], Fernanda V. Fernandez[6], Andrea X. Silva[7], Cristian Molina[7], Kenneth B. Storey[8], Francisco Bozinovic[2].*

[1]Instituto de Ciencias Ambientales y Evolutivas, Facultad de Ciencias, Universidad Austral de Chile, Valdivia, Chile.

[2]Center of Applied Ecology and Sustainability (CAPES), Facultad de Ciencias Biológicas, Universidad Católica de Chile, Santiago 6513677, Chile.

[3]Millennium Institute for Integrative Systems and Synthetic Biology (MIISSB), Santiago, Chile.

[4] The Swire Institute of Marine Science and School of Biological Sciences, The University of Hong Kong, Hong Kong SAR, China.

[5] CSIRO Oceans & Atmosphere, GPO Box 1538, Hobart 7001, TAS, Australia.

[6]Instituto de Fisiología, Facultad de Medicina, Universidad Austral de Chile.

[7]AUSTRALomics, Facultad de Ciencias, Universidad Austral de Chile.

[8]Department of Biology and Institute of Biochemistry, Carleton University, 1125 Colonel By Drive, Ottawa, Ontario K1S 5B6, Canada.

**Corresponding author*

robertonespolorossi@gmail.com

Formatted: Justified

Abstract

The small South American marsupial, *Dromiciops gliroides*, known as the missing link between the American and the Australian marsupials, is one of the few South American mammals known to hibernate. Expressing both daily torpor and seasonal hibernation, this species may provide crucial information about the mechanisms and the evolutionary origins of marsupial hibernation. Here we compared torpid and active individuals, applying high-throughput sequencing technologies (RNA-seq) to profile gene expression in three *D. gliroides* tissues and determine whether hibernation induces tissue-specific differential gene expression. We found 566 transcripts that were significantly up-regulated during hibernation (369 in brain, 147 in liver and 50 in skeletal muscle) and 339 that were down-regulated (225 in brain, 79 in liver and 35 in muscle). The proteins encoded by these differentially expressed genes ~~could~~ orchestrate multiple metabolic changes during ~~related to the hibernating~~hibernation ~~phenotype~~, such as inhibition of angiogenesis, prevention of muscle disuse atrophy, fuel switch from carbohydrate to lipid metabolism, protection against reactive oxygen species and repair of damaged DNA. According to the global enrichment analysis, brain cells seem to differentially regulate a complex array of biological functions (e.g., cold sensitivity, circadian perception, stress response); whereas liver and muscle cells prioritize fuel switch and heat production for rewarming. Interestingly, transcripts of thioredoxin interacting protein (*TXNIP*), a potent antioxidant, were significantly overexpressed during torpor in all three tissues. These results suggest that marsupial hibernation is a controlled process where selected metabolic pathways show adaptive modulation that can help to maintain homeostasis and enhance cytoprotection in the hypometabolic state.

Key words: hibernation, functional genomics, marsupials, adaptation, Dromiciops, RNA-seq.

1. Introduction

Endothermic animals (i.e., birds and mammals) produce metabolic heat in their bodies in a way that allows them to maintain a near-constant body temperature at values that are typically well above ambient temperature. This is an extravagant economy that requires these animals to maintain elevated energy budgets and spend a large part of their resources on basic maintenance ~~of endothermy~~. However, the benefits are large and allow endotherms to remain active in cold environments or travel long distances due to their high aerobic capacity, the only way to sustain long periods of activity (Koteja, 2004; Nespolo, Bacigalupe, Figueroa, Koteja, & Opazo, 2011). An adaptive strategy to ameliorate the high cost of endothermy is torpor, an energy-saving mechanism used by many small mammal and bird species, that involves a ~~controlled and~~temporal ~~reversible~~ interruption of endothermy that happens during cold periods (Boyer & Barnes, 1999; Ruf & Geiser, 2015). During torpor episodes, which can occur daily or seasonally (seasonal torpor is also known as hibernation, see reviews in ~~(~~Boyles et al., 2013; Ruf & Geiser, 2015), most ~~normothermic~~ normal biological functions are suppressed for periods ranging from overnight to several weeks. Animals show strong suppression of metabolic rate (often to values just 1-10% of ~~euthermic~~ active levels)(Ruf & Geiser, 2015), a decrease in body temperature to near ambient values, and experience reductions in~~a suppression of all~~ most physiological processes (e.g. strongly reduced heart beat and breathing rates). In these hypometabolic states, energy ~~expenditure is strategically redistributed~~ is re-allocated to some pathways that maintain organ function, whereas other processes ~~in a tissue specific manner where most of the energy is allocated to pro-survival pathways while all other processes a~~are suppressed or interrupted. For instance, the brain, an organ that cannot be shut down without serious damage, receives about 10% of its normal perfusion during

torpor but maintains neural activity, especially in the hypothalamus (Schwartz, Hampton, & Andrews, 2013). The liver, the metabolic center of the body, is also important during torpor as this organ processes nutrients, detoxifies reactive oxygen species (ROS) and disposes ~~of their damage~~toxic products, and produces multiple proteins and fuels for export to other tissues (Hadj-Moussa et al., 2016). Another important tissue, that shows reduced perfusion during torpor, is skeletal muscle. This tissue cannot be damaged ~~needs to be maintained,~~ as it is crucial for ~~arousal from hibernation and~~ rewarming ~~of~~ the body ~~through shivering thermogenesis~~during arousal from hibernation (Hindle, Karimpour-Fard, Epperson, Hunter, & Martin, 2011).

The state of suspended animation characterizing torpor and hibernation (i.e., the "hibernation phenotype", (Faherty, Villanueva-Canas, Klopfer, Alba, & Yoder, 2016) entails important risks for cells and tissues. A wealth of knowledge obtained from ~~eutherian~~ placental mammals~~models~~, for instance, has shown that torpor ~~hypothermia~~ increases the risk of cardiac arrest and since blood perfusion to peripheral organs can be reduced, tissues can become hypoxic and ischemic. This~~, which~~ in turn increases the risk of oxidative damage especially resulting from a massive production of ROS during ~~the~~ arousal ~~process~~ (Fons, Sender, Peters, & Jurgens, 1997; Rouble, Tessier, & Storey, 2014; Schwartz et al., 2013; van Breukelen, Krumschnabel, & Podrabsky, 2010). In the brain for instance, a reversible loss of synapses occurs, which reduces metabolic activity and helps to avoid the risk of neuronal death during torpor (Andrews, 2004 ; Schwartz et al., 2013). In skeletal muscle, adaptive mechanisms minimizing muscular disuse atrophy during torpor include differential regulation of genes related to protein biosynthesis and focal adhesion, which helps to maintain muscle integrity and contractibility (Andres-Mateos et al., 2012; Fedorov et al., 2014; Hadj-Moussa et al., 2016). Several detailed studies, all performed in placental

Formatted: Not Highlight

mammals (reviewed in ~~(~~Andrews, 2004; Carey, Andrews, & Martin, 2003; Morin & Storey, 2009; Villanueva-Canas, Faherty, Yoder, & Alba, 2014) have revealed that these changes involve ~~the crucial involvement of~~ transcriptional (gene-expression), post-transcriptional (non-coding RNA), translational (protein synthesis) and post-translational (reversible protein modification) changes ~~changes~~ assisting these pro-survival measures ~~during torpor~~. Here we present a case of massive transcriptional changes, many of them with adaptive significance, occurring in an hibernating species of marsupial.

Marsupials ~~("the alternative mammals"~~shared a last common ancestor with placental mammals approximately 160 million years ago (Graves & Renfree, 2013; Renfree, 1981) ~~-~~and since then, they have diversified into a wide range of ecological niches, especially after the colonization of Australia in the late-Cretaceous (Mitchell et al., 2014). Multiple small marsupial species exhibit torpor, which represents an evolutionary convergence with placental mammals ~~whose patterns and ecological significance have been studied in detail by several authors~~ (see ~~(~~Ruf & Geiser, 2015; Turner, Warnecke, Kortner, & Geiser, 2012). However, the underlying metabolic origins and patterns of marsupial hibernation are unclear. We know of three published studies describing some functional aspects of marsupial hibernation (Franco, Contreras, & Nespolo, 2013; Hadj-Moussa et al., 2016; Malan, 2010), which indicate some similarities with ~~eutherians~~ placental mammals (e.g., immunity suppression, mechanisms avoiding muscle atrophy, fuel switch to fat metabolism) but also some differences (e.g., a thermogenic role of the liver for rewarming and maintenance of the Akt metabolic pathway during torpor in the liver;~~)~~ ~~(~~Hadj-Moussa et al., 2016; Luu et al., 2018a; Villarin, Schaeffer, Markle, & Lindstedt, 2003). In this study, we used RNA-seq to analyze genomic-wide expression patterns of central and peripheral organs in the South American marsupial *Dromiciops gliroides* ~~In an attempt to gain a broad~~

~~overview of the gene expression changes associated with marsupial hibernation and thereby provide leads into the types of physiological and metabolic adaptations that marsupials experience during torpor, we have applied RNA-seq to analyze genomic-wide expression patterns of central and peripheral organs in the South American marsupial Dromiciops gliroides~~. This species is considered a "relict" mammal (sensu

~~*D. gliroides* is considered a relict species (~~Habel, Assman, Schmidtt, & Avise, 2010) as it belongs to ~~of the order~~ Microbiotheria, a formerly diverse group that diverged from Didelphimorphia (American marsupials) about 70 million years ago (MYA) and gave rise to Australidelphia, the large clade of Australian marsupials (Graves & Renfree, 2013; Mitchell et al., 2014). All Microbiotherids are extinct, excepting for *D. gliroides* (Palma & Spotorno, 1999).

According to Bozinovic et al. (2004), *D. gliroides* is one of the few South American mammals that exhibit ~~seasonal torpor or~~ hibernation (=seasonal torpor, ~~(~~ see also ~~(~~Geiser & Martin, 2013), but it also exhibits short torpor episodes during summer ~~experiencing torpor episodes of variable durations from a few hours in summer~~ (i.e., daily torpor) ~~to several months in winter~~ (Bozinovic, Ruiz, & Rosenmann, 2004; Nespolo, Verdugo, Cortes, & Bacigalupe, 2010). By the use of torpor, *D. gliroides* can save up to 60% of the energy that would otherwise be needed during the cold period. Previous work on *D. gliroides* suggested that torpor is associated with metabolic rate reductions of about 90% (Nespolo et al., 2010). During daily torpor episodes in *D. gliroides*, a drastic redistribution of blood in the body induces anemia, leukopenia, muscle atrophy and inflammation (Franco et al., 2013).

The apparently random patterns of torpor that *D. gliroides* exhibit were formerly interpreted as acute, uncontrolled responses to cold (Nespolo et al., 2010). However, a

Formatted: Font: Italic

Formatted: Font: Not Italic

Formatted: Font: Italic

number of recent discoveries have changed this view. For instance, *D. gliroides* seems to anticipate the cold season as a response to photoperiodic changes and thermal acclimation (Franco, Contreras, Place, Bozinovic, & Nespolo, 2017). In addition, several torpor-regulation mechanisms were described in this species, including differential expression microRNAs (Hadj-Moussa et al., 2016), implementation of the stress response through MAPK signaling (Luu et al., 2018b; Wijenayake et al., 2018a), reorganization of fuel use (Wijenayake et al., 2018b), and partial suppression of protein synthesis (Luu et al., 2018a). Here we present a comprehensive transcriptomics analysis of torpid *D. gliroides*, providing the first explicit description of differentially regulated metabolic pathways of marsupial hibernation. ~~{Franco, 2017 #9553}~~

~~{Hershkovitz, 1999 #9603}By the use of torpor, *D. gliroides* can save up to 60% of the energy that would otherwise be needed during the cold period. Previous work on *D. gliroides* suggested that torpor is associated with metabolic rate reductions of about 90% {Nespolo, 2010 #3064}. During daily torpor episodes in *D. gliroides*, a drastic redistribution of blood in the body induces anemia and leukopenia, and probably muscle atrophy and inflammation {Franco, 2013 #3937}. A series of recent biochemical studies revealed that torpor in *D. gliroides* is a precisely controlled condition where metabolic reorganization and proper hepatic and muscle function are maintained. Regulatory mechanisms involved include differential expression microRNAs {Hadj-Moussa, 2016 #9113}, implementation of the stress response through MAPK signaling and other pro-survival mechanisms {Luu, 2018 #9897;Wijenayake, 2018 #9895}, reorganization of fuel use {Wijenayake, 2018 #9894}, and contrary to what is known in eutherian mammals, *D. gliroides* does not seem to suppress protein synthesis during torpor {Luu, 2018 #9896}.~~

Formatted: Font: Italic

Formatted: Justified, Indent: First line: 0.49"

2. ~~Materials and methods~~Methods

Formatted: Justified

2.1 Animal collection and laboratory treatment

D. gliroides is one of the four marsupial species of Chile; it is an omnivorous, nocturnal, opossum-like mammal with arboreal adaptations (i.e., opposable thumbs, prehensile tail and eyes in frontal plane) (Hershkovitz, 1999). This species is strongly associated with the temperate rainforest, where temperatures fluctuate between 5 and 25ºC (Franco et al., 2017). In this ecosystem, ~~W~~we captured thirteen adult *D. gliroides* (7 males; 6 females), particularly in the Southern part of Valdivia, Chile (39°48′S, 73°14′W; 9 m.a.s.l.) during the austral summer (January-February) in 2014, using Tomahawk traps located in trees 1m above ground, baited with bananas and yeast. Upon capture, individuals were immediately transported to the laboratory where they were housed in plastic cages of 45x30x20 cm^3 with 2 cm of bedding. All individuals were maintained in a climate controlled chamber (PiTec Instruments, Chile) at 20±1°C and with a 12 h: 12 h photoperiod for two weeks. Animals were fed a mix of mealworms, fruits, and water ad libitum. After two weeks of acclimation, and after checking that each animal had increased body mass, individuals were randomly assigned to two groups: torpor (3 males, 4 females) and active controls (3 males, 3 females). Active animals were sampled from the above conditions. To induce torpor, and to avoid any injury, animals were subjected to a gradual decrease of ambient temperature (−1 °C every 20 min) until 10 °C was reached (photoperiod was maintained as initially). To minimize animal disturbance during the experimental trials, torpor incidence was verified by visual observation several times a day between 09:00–17:00. In this species torpor can be easily identified: animals are not responsive when the cage is gently moved and breathing frequency is below three breaths per minute. After declaring torpor for a given individual, the animal was continuously monitored by visual

inspection every four hours, during~~for~~ four consecutive days to ensure that torpor was sustained; and individuals were then euthanized. Euthanasia followed protocols approved by the Committee on the Ethics of Animal Experiments of the Universidad Austral de Chile. Tissue samples were excised in less than a minute and immediately frozen in liquid nitrogen. All ~~animal~~animals capture, handling and maintenance procedures followed the guidelines of the American Society of Mammalogists (Gannon, Sikes, & Comm, 2007) and were authorized by the Chilean Agriculture and Livestock Bureau (SAG: Servicio Agrícola y Ganadero de Chile, permit No. 1054/2014 and 1118/2015).

2.2 RNA extraction, cDNA library construction and sequencing

Total RNA was extracted from brain, liver and skeletal muscle from the hind leg (thigh) of each animal using the NucleoSpin RNA II Macherey Nagel kit (Bethlehem, PA, USA) and additional DNAase, following manufacturer's instructions. The quality of the obtained RNA was assessed by an Agilent 2100 Bioanalyzer. Only high-quality RNA with RNA integrity numbers (RINs over 7.5) was used (13 for brain, 6 for liver and 4 for skeletal muscle; 1:1 ratio of torpor: active organisms). RNA quantity was estimated using the Kit Quant-iTTM RiboGreen® RNA in a DQ300 Hoefer fluorometer. Individual cDNA libraries (N=25) were labeled with sample-specific barcode adaptors, normalized and randomly built using the TrueSeq RNA Sample Preparation Kit v2 (Illumina; 0.5 µg of total RNA), following manufacturer's recommendations. These cDNA libraries were then pooled in equimolar ratios, with 2 or 3 randomly selected samples per pool, and were sequenced (2 × 150 bp PE) in eleven separated Illumina MiSeq runs at the AUSTRAL-*omics* Core Facility, Facultad de Ciencias, Universidad Austral de Chile (www.australomics.cl). Randomization of library preparation and sequencing is described

as a way to avoid confounding experimental factors with technical factors (Conesa et al., 2016). Sequences were demultiplexed based on their sample-specific barcode adaptors. Raw data from the sequencing runs were deposited at the Sequence Read Archive (SRA) repository of the National Center for Biotechnology Information (NCBI) under accession number SRR6255590- SRR6255614 of the Bioproject PRJNA416414. We eliminated samples with RIN values below 7.0, which happened especially with skeletal muscle and resulted in unbalanced final sample sizes among tissues.

2.3 Bioinformatics

Following sequencing, quality control (filtering and trimming) of the raw data was performed using the Trimmomatic tool v.030 (Bolger, Lohse, & Usadel, 2014) ~~with~~ and we removed every read with a phred quality score ~~=~~ of 30 or less, which gives 99.9% in base accuracy~~(every read with less than a value of 30 bp was removed)~~. We used this phred score to be conservative and avoid multiple mappings, which could produce isoforms as artifacts of incorrect mismatches (see a debate in ~~(~~Williams, Baccarella, Parrish, & Kim, 2016). Still, some isoforms were produced which we interpret according to the involved biological function~~as a biological factor (see Discussion)~~. The quality trimmed reads were assembled using Trinity 2.0.4 (Grabherr et al., 2011) with the standard Inchworm, Chrysalis and Butterfly pipeline and a minimum contig length of 200 nt (De Wit et al., 2012). These setting parameters have been optimized for de novo assemblies of non-model species with Trinity (Grabherr et al., 2011)~~(De Wit et al., 2012)~~. Duplicate sequences were then removed manually~~after *de novo* assembly~~. The quality and completeness of the ~~this~~ assembly ~~were~~was analysed using the software QUAST for assembly statistics ~~(Gurevich *et al.* 2013)~~(Gurevich, Saveliev, Vyahhi, & Tesler, 2013), and by mean of the Benchmarking

Universal Single-Copy Orthologs (BUSCO v.3) approach (Simao, Waterhouse, Ioannidis, Kriventseva, & Zdobnov, 2015) ~~(Simão et al., 2015)~~. For BUSCO, our analyses were based on a subset of 233 (Core Vertebrate Genes, CVG) and 4104 (Mammalia) orthologs, which in eukariotes are widely conserved core genes that generally lack paralogs ~~in the eukaryotes~~ (Simão et al., 2015).

Processed high quality reads were mapped to the assembled contigs using the Bowtie (version 2.0) read aligner (Langmead & Salzberg, 2012). To improve isoform counts, we used the RNA-Seq by Expectation Maximization (RSEM, version 1.0) software (Li & Dewey, 2011) that assesses transcript abundance in the assembled transcriptome. Then, a sample-based clustering analysis (heatmap of Euclidean distances) was performed in order to identify the distribution of the samples according to the experimental conditions using the R function *dist* and the function *heatmap.2* from the gplots package. Our de novo assembled transcriptome was blasted against the UniProt (Swiss-Prot and TrEMBL), KOBAS and NCBI RefSeq (nr) protein databases using the BLASTX algorithm with an e-value cutoff of $1e^{-5}$ (Altschul, Gish, Miller, Myers, & Lipman, 1990). With this procedure, the annotation was performed against a database containing several million proteins. Annotated unigenes (consensus, non-redundant sequences) were further searched for Gene Ontology (GO) terms using Blast2GO software **(www.blast2go.com)**(Conesa et al., 2005) according to the main categories of Gene Ontology (GO; molecular functions, biological processes and cellular components) (Ashburner et al., 2000). Complementary annotations were done with the InterProScan v.5 software (Jones et al., 2014), which provides functional analysis of proteins by classifying them into families and predicting domains and important sites. The annotation results were further fine-tuned with the Annex and GO slim functions of the Blast2GO software in order to improve and summarize the functional

information of the transcriptome dataset. Additionally, proteins were finally annotated using the Kyoto Encyclopedia of Genes and Genomes (KEGG) and its automated assignment server (KAAS) (Moriya, Itoh, Okuda, Yoshizawa, & Kanehisa, 2007).

2.4 Differential gene expression analysis

Differentially expressed genes (DEGs), were identified using the R/Bioconductor package DESeq2 v.1.10 (Love, Huber, & Anders, 2014) with raw read counts. The estimated counts were normalized against the size of the transcriptome and the total number of readings that were mapped per sample, using the regularized logarithm (rlog) method in DESeq2 and expressed in a log2 scale. Basically, DESeq2 normalizes the counts by dividing each column of the count table (samples) by the size factor of this column. The size factor is then calculated by dividing the samples by the geometric means of the genes, which brings the count values to a common scale suitable for comparison (Love et al., 2014). P-values for differential expression were calculated using a negative binomial test for differences between the base means of the control and torpor conditions. The P-values were adjusted for multiple test correction using Ward's method with the Benjamini-Hochberg procedure (Ferreira & Zwinderman, 2006). Significant DEGs were defined as those genes with an adjusted p-value (false discovery rate, FDR) ≤ 0.05 and $\log_2$ (fold change) ≥ 1. Differentially expressed genes across samples were visualized using standard volcano plots, where $\log_2$ fold change was plotted against $\log_{10}$ (FDR adjusted p-value). Furthermore, heatmaps were produced to visualize gene expression across samples and tissues using z-scores (based on normalized counts) and plotted with the Heatmapper software (Babicki et al., 2016).

Enrichment of GO and KEGG pathways in genes up- and down-regulated during torpor were analyzed using Blast2GO (Fisher's exact test) and the goseq R package (Young, Wakefield, Smyth, & Oshlack, 2010), with a threshold false discovery rate of 0.001. The reference used was the whole transcripts with GO slim annotation. Chord diagrams to visualize enriched pathways were drawn using Circos (Krzywinski et al., 2009).

3. Results

In this study, a total of 414 million of reads were generated from 23 libraries derived from brain (13), liver (6) and skeletal muscle (4) of active and hibernating *D. gliroides* (mean = 8.6 million of reads per sample; see Supplementary Table 1~~file~~). After a stringent filtering process, ~94% high-quality, adapter-free and non-redundant reads were retained for further downstream analyses. Our *de novo* assembly generated 507,815 contiguous sequences (putative transcripts, contigs) with a mean sequence length of 718 bp, an N50 of 1,387 bp and an L50 of 6,0430. The longest sequence contains 68,683 bp and 16% of the sequences were over 1k bp. The assessment of transcriptome completeness using the Benchmarking Universal Single-Copy Orthologs (BUSCO) approach, identified a high representation of Core Vertebrate Genes (CVG), with 94.4% marked as complete and 98.1% as complete + partial. Only 1.29% of the CVG were missing. Similarly, our BUSCO analysis revealed 3,577 (87%) complete and 3,929 (95.74%) complete + partial Mammalian Core Genes (MCG). From this reference gene set, 175 (4.26%) MCG were missing in our *de novo* assembly. In terms of the functional association of the putative transcripts in the *de novo* assembled transcriptome of *D. gliroides*, our analysis produced 31,438 contigs that were blasted to known proteins in the public databases NCBI (nr),

Formatted: Not Highlight

Formatted: Not Highlight

KOBAS and UniProt (Swiss-Prot and TrEMBL)~~,~~ ~~and~~ were linked to GO classifications (average 4.55 GOs per contig). Hypothetical or predicted proteins in these databases were excluded by discarding matches associated to "hypothetical", "predicted", "unknown" and "putative" categories. Most of the annotated contigs (93%) hit against the koala (*Phascolarctos cinereus*), the gray short-tailed opossum (*Monodelphis domestica*) and the Tasmanian devil (*Sarcophilus harrisii*) genomes, in ~~that~~this ~~hierarchical~~ order.

Our transcriptomic survey of hibernating *D. gliroides* identified 73,125 mRNA transcripts in the brain, of which 594 exhibited differential regulation during torpor; 225 of them were down-regulated and 369 up-regulated (Fig 1A). Some of the very highly differentially expressed genes are named on the figure~~1~~. In the liver, we identified 36,865 transcripts with 226 showing differential regulation during torpor: 79 down-regulated and 147 up-regulated (Fig 1B). In skeletal muscle, these numbers were 13,038 total transcripts with 85 differentially regulated during torpor: 35 down-regulated and 50 up-regulated (Fig 1C). We found 317 transcripts that were exclusively up-regulated in the brain, 131 transcripts that were exclusively up-regulated in the liver, and 44 transcripts exclusively up-regulated in muscle (Fig. 1D; upper panel). Oppositely, 191 transcripts were exclusively down-regulated in the brain, 73 in the liver and 46 in muscle (Fig. 1D; lower panel). A few transcripts were up-regulated or down-regulated in common among two or all three of the organs; these are named in Fig 1D and more details about their functions are given in Supplementary Tables ~~A1-A6~~2 to 7. For example, *SETDB1, SCL25A18 and ACADVL* were up-regulated in both brain and liver whereas *EIF2AK1* was up-regulated in both brain and muscle. Only one transcript, encoding thioredoxin-interacting protein (*TXNIP*; Fig 1), was up-regulated in common in all three tissues and also fell within the top ten upregulated genes in each of these organs (see Supplementary Tables). This gene is described as

encoding potent antioxidant protein associated with a number of human diseases ~~(Yoshioka, 2014 #9855;Spindel, 2012 #9856)~~ (see Discussion).

~~For simplicity, our further analysis focused on the top ten differentially regulated genes in each tissue (Figs 2-4). Comparisons of gene expression as the number of transcripts per million (TPM) between torpid and active individuals are shown in Figs 2 to 4 for the top five up-regulated and top five down-regulated genes in each organ.~~ Functions such as protection against reactive oxygen species (gene: *TXNIP*; overexpressed in all three organs of hibernators: Fig 1A-C; Fig 2A~~, Fig 4B; Supplementary Tables A1, A3, A5~~), inhibition of transcription (genes: *HIST2H2A*; *SRSF5*; Fig 1A, Fig 2~~e,g~~), fuel switch to fat metabolism (genes: *ZNF638, ATG3*; Fig 1D,F; Fig 2) and inhibition of angiogenesis (*ANGPTL4*; Fig 1C), appeared as the most important changes in the brain (Fig 1; Supplementary Tables 2 and 3~~A1, A2~~). In the liver, the greatest changes in gene expression characterizing torpor seemed to be associated with the fuel switch from carbohydrate to lipid catabolism, since four genes involved in promoting fat catabolism enzymes ~~(see Table A5)~~ were among the top five differentially expressed ones (*PDP2, CYB5R3*, overexpressed; *NR1H4, ND4,* under-expressed, Suppl. Table 4 and 5~~; Fig 3D-J; Supplementary Table A3, A4~~). In muscle, a similar interpretation indicated that mechanisms for avoiding muscle atrophy (over-expressed genes: *PVALB, EIF3D, GADPH*, Fig 4A-E; Supplementary Tables 4 and 5~~ A5, A6~~) may be the most important functions being ~~emphasized~~ exacerbated during torpor.

A functional enrichment analysis based on the gene-ontology database (GO) suggested that several metabolic pathways were enriched (both under-expressed and over-expressed) in the brain during torpor, compared with the other two organs, that only showed overexpression of a few biological functions (Fig 2~~5~~A). This is also appreciated in

the expression profiles of each organ (i.e., the "heatmaps", see Supplementary Fig 4~~A1~~). The analysis arising from the Kyoto Encyclopedia of Genes and Genomes (KEGG) showed a myriad of functions that were differentially regulated in the brain, such as cold sensitivity, circadian perception, mRNA surveillance, and stress response (Fig 2~~5~~B). The liver and muscle profile, by contrast, indicated that the most important modified functions were orientated to the maintenance of organ function (e.g., biosynthesis of amino acids) and to fuel switch to lipid metabolism (e.g., fatty acid degradation, metabolic pathways) (Fig 2~~5~~C, D).

4. Discussion

Today, comparative physiologists have a broad repertoire of technological tools that can be used to identify functional changes associated to a given physiological condition; from simple (and often inexpensive) measures of whole-animal metabolic fluxes (e.g., respirometry, blood biochemistry and haematology, tissue-specific enzymes and metabolites; see recent examples in ~~(~~Franco et al., 2013; Il'ina et al., 2017; Rouble & Storey, 2015) to the powerful characterization of exacerbated/enriched metabolic pathways that high throughput sequencing methods ~~or proteomics analyses (e.g. mass spectrometry)~~ provide. ~~Here~~ To the best of our knowledge, this is the first~~we used mRNA sequencing~~ RNA-seq analysis of ~~(RNA-seq) to identify genes that were differentially expressed during~~ hibernation in a marsupial, which provided a wealth of detailed information ~~species~~. In order to avoid being "lost in the map" ~~of molecular details~~ (sensu ~~(~~Travisano & Shaw, 2013), we ~~will~~ focus on some particularly ~~interesting differentially~~important metabolic functions with relevance for torpor, provided by our de novo assembly. This procedure ~~expressed genes from the top ten lists of each tissue, explore their potential relevance to~~

Formatted: Justified, Indent: First line: 0"

~~torpor and, where applicable, associate these functions with previously described phenomena of the hibernation phenotype in eutherians or in *D. gliroides*. For reference, descriptions of the known functions of the mammalian proteins encoded by the top ten differentially regulated genes in each tissue are provided in Supplementary Tables A1-A6.~~ showed high completeness as evidenced for the percentage of coverage of Core Vertebrate Genes (CVG) and Mammalian Core Genes (MCG). The overall statistics of our assembly (N50, L50, contig length, number of contigs >1k), were similar to the results documented in *de novo* assembled transcriptomes of other mammals, such as the beaver (*Castor fiber L.*; testis; ~~(~~Bogacka et al., 2017), and the Nile grass rat (*Arvicanthis ansorgei*; retina; ~~(~~Liu et al., 2017). However, we had higher values compared with marsupials such as the long-nosed bandicoot (*Perameles nasuta*; heart, liver, spleen and kidney; ~~(~~Morris et al., 2018), and the Virginia opossum *Didelphis virginiana*; kidney; ~~(~~Eshbach et al., 2017).

4.1 Thioredoxin interacting protein and oxidative damage

The most notable finding of our analysis was the overexpression in all three organs of *TXNIP*, the gene encoding thioredoxin interacting protein. ~~TXNIP was significantly overexpressed by five-fold in the brain (log fold change = 2.42, see Table A1), 65.5-fold in liver (log fold change = 6.0, see Table A3), and 68.1 fold in skeletal muscle (log fold change = 6.1, see Table A5), suggesting an important role for its protein product (TXNIP) in marsupial hibernation. TXNIP~~The TXNIP was first identified as an endogenous negative regulator of thioredoxin, a ubiquitous redox protein in cells that is particularly involved in the reduction of oxidized cysteine residues and cleavage of disulfide bonds (Nishiyama et al., 1999). ~~Thioredoxin also displays radical scavenging activity and facilitates hydrogen peroxide breakdown via thioredoxin peroxidases and peroxiredoxins {Nishiyama, 1999~~

Formatted: Font: Not Italic

Formatted: Justified

Formatted: Font: Italic

Formatted: Font: Italic

Formatted: Font: Not Italic

Formatted: Font: Not Italic

#9893}. TXNIP has been linked, not just with an antioxidant/redox role (e.g. to minimize ischemia-reperfusion damage), but with the broader regulation of mitochondrial function to help suppress oxidative metabolism when oxygen is limiting, and shift metabolism to anaerobic glucose catabolism by mediating inhibition of pyruvate dehydrogenase (Chong et al., 2014; Spindel, World, & Berk, 2012; Yoshioka & Lee, 2014). Several diseases are associated with disruptions of the thioredoxin system, such as cataract formation, ischemic heart diseases, several cancers, diabetes complication and hypertension (Maulik & Das, 2008). TXNIP is also involved in inhibiting unnecessary glucose influx into cells while also promoting fatty acid oxidation (Hand et al., 2013) (57); both of these are central features of a hibernating phenotype. Indeed, recent research has shown that TXNIP has a role to play in torpor; the *TXNIP* gene was overexpressed in brain (hypothalamus), liver, and white and brown adipose during induced-torpor experiments in mice as well as in natural torpor in Siberian hamsters, suggesting a possible universal role of its protein product in hibernation (*Phodopus sungorus*)(DeBalsi et al., 2014; Hand et al., 2013; Jastroch et al., 2016). Our current identification of a multi-organ strong upregulation of *TXNIP* in *D. gliroides* (including multiple gene variants in brain) adds further support for the proposal that TXNIP has a central role to play in the metabolic control during of torpor., including in both eutherian and marsupial hibernators, and that it deserves concerted further study.

Formatted: Highlight

Analysis of differentially expressed genes in three different tissues of *D. gliroides* provided multiple intriguing insights into the potential metabolic adaptations that support hibernation in this small marsupial. Top differentially expressed genes in brain are shown in Fig. 2 and Table A1 and A2 and, apart from *TXNIP* (already discussed), offer three notable upregulated genes that are particularly interesting. One is *RPS3* that encodes a 40S ribosomal protein S3 (Table A1) that is well known for its role in ribosomal biogenesis.

Formatted: Justified, Indent: First line: 0.49"

~~However, more recent studies have shown that when ROS levels rise in cells, RPS3 migrates into the mitochondria where it assists in the repair of oxidative damage to mitochondrial DNA {Kim, 2013 #9899}. Its simultaneous loss from the cytoplasm leads to suppression of ATP-expensive protein synthesis under these stress conditions, adding another layer of translational suppression to the known controls on eIF2a, 4E-BP1 and eEF2 that inhibit ribosome assembly in eutherian hibernators. A mitochondrial role for RPS3 could be important to stabilizing the mitogenome during prolonged torpor and may be crucial during the arousal process when mitochondria go into "overdrive" in their consumption of oxygen to support shivering or nonshivering thermogenesis.~~

4.2 Metabolic switch

In the brain, ANGPTL4 secretion (which we found strongly up-regulated) is of central importance in regulating the switch to a lipid-based fuel economy during torpor, facilitating lipid release from adipose and uptake by other tissues. Indeed, recent studies have reported significant upregulation of *ANGPTL4* transcripts in ground squirrel heart during torpor and interbout arousal stages of hibernation as compared with pre- or post-hibernation months (Vermillion, Anderson, Hampton, & Andrews, 2015) as well as during torpor in a ground squirrel bone-marrow transcriptome when compared with summer animals (intermediate transcript levels were seen during interbout arousal) (Cooper et al., 2016). In the same vein, a powerful indicator of the suppression of carbohydrate fuel use within the brain during torpor is pyruvate dehydrogenase kinase 4 (*PDK4*), whose transcripts were strongly elevated in the brain. Phosphorylation of pyruvate dehydrogenase (PDH) at S232, S293 or S300 by any of four PDK isozymes inhibits its activity (Harris, Bowker-Kinley, Huang, & Wu, 2002) and is crucial for blocking the oxidation of pyruvate as a substrate, especially when carbohydrate reserves must be conserved. Indeed, strong

Formatted: Indent: First line: 0.49"

suppression of PDH activity during hibernation has been widely reported in multiple tissues of eutherian hibernators (summarized in (Wijenayake, Tessier, & Storey, 2017). Strong increases in PDH phosphorylation at 1, 2 or all 3 serine sites were also reported for six tissues (including brain, liver and skeletal muscle) of *D. gliroides* (Wijenayake et al., 2017) and the upregulation of *PDK4* in brain (predictably elevating PDK4 protein) would support PDH inhibition and presumably help to direct brain to make greater use of ketones as substrates during hibernation.

4.3 Marsupial nonshivering thermogenesis

Uniquely in marsupials, liver appears to be the main site of nonshivering thermogenesis since brown adipose tissue is not present (Jastroch, Wuertz, Kloas, & Klingenspor, 2005; R. W. Rose, West, Ye, McCormack, & Colquhoun, 1999) and, hence, modulation of multiple controls on lipid metabolism is probably needed to regulate this novel liver function (Hadj-Moussa et al., 2016). Among down-regulated genes we found in liver, three deserve particular mention for their potential roles in the hibernating marsupial: *ND4, NR1H4* and *TCAF2* (see Supplementary Table 5). Transcript levels of the mitochondria-encoded NADH dehydrogenase subunit 4 (*ND4*) gene were strongly reduced in *D. gliroides* liver during hibernation. By contrast, strong increases in ND4 expression were reported in brown adipose tissue of the bat, *Myotis lucifugus* during hibernation (Eddy, Morin, & Storey, 2006) and *ND2* transcripts (also mitochondria-encoded) were elevated during hibernation in heart and skeletal muscle of 13-lined ground squirrels, *Spermophilus tridecemlineatus* (Fahlman, Storey, & Storey, 2000). Compared with *D. gliroides*, this suggests that there may be either tissue-specific (liver versus muscle/BAT) or marsupial vs eutherian differences in the reorganization of mitochondrial oxidative

metabolism in the torpid state. On the other hand, *NR1H4* encodes the NR1H4 protein (nuclear receptor subfamily 1, group H, member 4) that is also known as the bile acid receptor (BAR) or the farnesoid X receptor (FXR). This receptor is a master regulator of hepatic triglyceride, cholesterol and bile acid metabolism. Active FXR exerts controls that suppress *de novo* lipogenesis and promote FFA oxidation. FXR gene expression was also reduced in liver of hibernating ground squirrels compared with summer animals (Nelson, Otis, & Carey, 2009) and also occurs in non-alcoholic fatty liver disease in humans. FXR-deficient mice not only exhibited marked hepatosteatosis (fatty liver) and hypertriglyceridemia (Jiao, Lu, & Li, 2015; Wollam & Antebi, 2011) but showed an accelerated fasting-induced entry into torpor and markedly greater cold-intolerance as compared with controls (Cariou et al., 2007). Hence, the strong suppression of *NR1H4* transcript levels (implying suppressed FXR protein levels) in liver of hibernating *D. gliroides*, suggests a role for this receptor in the management and/or restructuring of liver lipid metabolism during hibernation when fatty acid oxidation is the primary mode of ATP production~~(Zietak, Chabowska-Kita, & Kozak, 2017)~~. This, together with previous results in *D. gliroides* and also in *Monodelphis domestica* (Hadj-Moussa et al., 2016; Villarin et al., 2003) provides an intriguing role between FXR (BAR) function, lipid metabolism and NST in the liver metabolism of hibernating marsupials.

~~(Eddy, Morin, & Storey, 2006)(Fahlman, Storey, & Storey, 2000)Damage done by accompanying high levels of free radicals generated during arousal could require immediate DNA damage repair. In general, some themes were seen. For example, the genes for several mRNA splicing factors and related proteins were downregulated (*SRSF5*, *SF3A1*, *SRSF5* in brain, *SREK1* and *THOC5* in liver) although one was upregulated in liver~~

Formatted: Highlight

Formatted: Justified, Indent: First line: 0.49"

Formatted: Highlight

~~(*DHX38*, an ATP-dependent RNA helicase) as was *SCL25A* in both brain and liver. Reduced expression of these factors could contribute to a general suppression of gene transcription in the hypometabolic state of hibernation, as has been reported from other types of evidence for various eutherian hibernators (Storey & Storey, 2010)(Luu et al., 2018a). Furthermore, the shared upregulation of *SETDB1* (encoding a histone lysine methyltransferase that supports transcriptional suppression) is a further indication of global transcriptional controls during hibernation whereas upregulation of *EIF2AK1* (a kinase that inhibits the eukaryotic initiation factor 2) in both muscle and brain is a strong indicator of the comparable inhibition of ribosomal mRNA translation{Hawkins, 2018 #9955}. us that active suppression of metabolic activities are occurring through inhibition of (Hawkins & Storey, 2018)~~

4.5 KEGG integrated analysis

The analysis based on the Kioto Encyclopedia of Genes and Genomes (KEGG, see Fig 2B) showed, in torpid animals, overexpression of multiple genes contributing to the mTOR signaling pathway (genes *SEH1L*, *SGK1*), circadian rhythm pathways (genes *CUL1*, *CRY2*), notch signaling pathway (genes *NCOR2*, *DTX3*, *EP300*), and ubiquitin-mediated proteolysis (genes *CUL1*, *UBE20*, *CDC34*, *UBA3*, *HUWE1*). ~~The~~ Seh1 (known as SEH1L in mammals) is a subunit of the GATOR2 complex that is an essential activator of mTORC1 kinase. Seh1 is also a subunit of the Nup107 complex (the nucleoporin Y-complex) that plays a major role in formation of the nuclear pore complex in interphase and associates with kinetochores in mitosis (Platani, Samejima, Samejima, Kanemaki, & Earnshaw, 2018). SGK1, on the other hand, is one of many downstream targets of the mTOR C2 kinase, representing one arm of the mTORC2 signaling pathway (Garcia-

Formatted: Justified

Formatted: Justified, Indent: First line: 0"

Formatted: Justified

Martinez & Alessi, 2008). Cry2 is one of the main circadian rhythm proteins, and it is known that this protein is upregulated during hibernation in hamsters and ground squirrels (Crawford et al., 2007).

The high level of transcriptional activity detected in the brain contrasts with the few enriched pathways of liver and muscle (Fig 2C and D). This, however, could be a consequence of the low sample size we had for those two organs (especially for muscle), which makes our conclusions regarding these organs, preliminary. Both for liver and muscle we found a strong differential regulation (up- and down--regulation) of metabolic pathways *sensu lat~~t~~o*, which is probably due to the physiological switch from carbohydrate to lipid-based metabolism also described in other hibernators (Boyer & Barnes, 1999; Storey & Storey, 2010; Villanueva-Canas et al., 2014), and in *D. gliroides* (Wijenayake et al., 2018b). This is confirmed here, as we found strong overexpression of pathways related ~~with~~to fatty acid degradation (genes *ACSL5, ACA*DVL) and regulation of autophagy (genes *ULK1, ULK2, GABARAPL1*) in the liver (see Fig 2C). Hibernators all increase their content of unsaturated FAs so that lipid depots can remain fluid at low Tb (Contreras, Franco, Place, & Nespolo, 2014; J. C. Rose, Epperson, Carey, & Martin, 2011). Our findings ~~here~~ support this view, ~~a~~since differential up-regulation of ACSL5 (the protein acyl-CoA synthetase long-chain 5) is used both in fatty acid synthesis and beta-oxidation.

By contrast, in muscle we found overexpression of the longevity-regulating pathway, which indicates that differentially expressed genes in the muscle are directed toward the maintenance of organ function, which in marsupials (in addition to the liver, as discussed before) is crucial for rewarming ~~during arousal from torpor~~(Hadj-Moussa et al., 2016; Opazo, Nespolo, & Bozinovic, 1999).

Formatted: Font: Italic

Formatted: Not Highlight

Formatted: Not Highlight

5. Summary and conclusions

In this paper, we have shown that the hibernating marsupial *D. gliroides* express adaptive physiological mechanisms to deal with the consequences of hypometaboism and cold during torpor. These mechanisms are tissue-specific and involve: (1) protection against reactive oxygen species, ROS (i.e., oxidative damage) by overexpressing the *TXNIP* gene among others, (2) metabolic switch from carbohydrate to fat-based metabolism in liver and muscle, (3) nonshivering thermogenesis in the liver, (4) transcriptional suppression of non-essential functions, (5) overexpression of proteins controlling circadian rhythm in the brain, and (6) overexpression of longevity-regulated pathways that maintain organ function in muscle. In terms of survival and fitness, these physiological changes have the net consequence of making this metabolic depression, reversible and safe. Several of these mechanisms are conserved, previously described in placental mammals~~(Jastroch et al., 2016; van Breukelen & Martin, 2015)~~, but also described in *D. gliroides*. Some of them are apparently unique to marsupials (e.g., role of liver in rewarming), but still only described in a few species. Given that ~~(Hadj-Moussa et al., 2016; Luu et al., 2018a; Luu et al., 2018b; Wijenayake et al., 2018a; Wijenayake et al., 2018b)~~Microbiotherids are considered the ancestors of Australian marsupials (Mitchell et al., 2014), further studies in other marsupial species would be crucial to determine the generality of our findings.

~~{Mitchell, 2014 #8870}~~

~~Our de-novo assembly showed high completeness as evidenced for the percentage of coverage of Core Vertebrate Genes (CVG) and Mammalian Core Genes (MCG). These values as well as the overall statistics of our assembly (N50, L50, contig length, number of contigs >1k), were similar to the results documented in *de-novo* assembled transcriptomes of mammals such as beavers (*Castor fiber L.*; testis; {Bogacka, 2017 #9964}~~Bogacka et al.,

Formatted: Justified

Formatted: Justified, Indent: First line: 0.49"

Formatted: Font: Italic, Highlight

Formatted: Highlight

Formatted: Justified

2017), and the Nile grass rat (*Arvicanthis ansorgei*; retina;*{Liu, 2017 #9965}* Liu et al., 2017), but higher than marsupial de novo assemblies including the long-nosed bandicoot (*Perameles nasuta*; Heart, liver, spleen and kidney; {Morris, 2018 #9966}Morris et al., 2018), and the Virginia opossum (*Didelphis virginiana*; kidney; {Eshbach, 2017 #9967}Eshbach et al., 2017).

Reference:

Bogacka, I., Pauksztо, L., Jastrzębski, J. P., Czerwińska, J., Chojnowska, K., Kamińska, B., ... & Kamiński, T. (2017). Seasonal differences in the testicular transcriptome profile of free-living European beavers (Castor fiber L.) determined by the RNA-Seq method. PloS one, 12(7), e0180323.

Liu, M. M., Farkas, M., Spinnhirny, P., Pevet, P., Pierce, E., Hicks, D., & Zack, D. J. (2017). De novo assembly and annotation of the retinal transcriptome for the Nile grass rat (Arvicanthis ansorgei). PloS one, 12(7), e0179061.

Morris, K. M., Weaver, H. J., O'Meally, D., Desclozeaux, M., Gillett, A., & Polkinghorne, A. (2018). Transcriptome sequencing of the long-nosed bandicoot (Perameles nasuta) reveals conservation and innovation of immune genes in the marsupial order Peramelemorphia. Immunogenetics, 70(5), 327-336.

Eshbach, M. L., Sethi, R., Avula, R., Lamb, J., Hollingshead, D. J., Finegold, D. N., ... & Weisz, O. A. (2017). The transcriptome of the Didelphis virginiana opossum kidney OK proximal tubule cell line. *American Journal of Physiology-Renal Physiology*, *313*(3), F585-F595.

Formatted: Justified, Indent: First line: 0"

Formatted: Justified

Acknowledgements. This study was funded by Fondo Basal CAPES 0002-2014 to Francisco Bozinovic and MIISSB Iniciativa Científica Milenio (MIISSB). Juan Diego Gaitan acknowledges a CSIRO-OCE postdoctoral fellowship. Julian F. Quintero-Galvis acknowledges a Conicyt PhD fellowship N° 21160901. Roberto Nespolo acknowledges a Fondecyt grant N° 1180917. Andrea Silva acknowledges a Fondecyt grant N° 11140680. Kenneth B. Storey acknowledges NSERC Canada grant No 6793.

Author contributions

R.F.N designed the study, contributed to the experiment execution and wrote the manuscript. J.D.G-E contributed with the experiment design, contributed to the experiment execution, performed the final bioinformatic analysis and contributed with manuscript editions. J.F.Q-G collaborated with the experiment, contributed with data analysis and contributed with manuscript editions. F.V.F contributed with manuscript editions and data analysis. A.X.S contributed to the experiment execution and with the bioinformatic analysis. C.M performed the initial bioinformatic analysis and contributed with manuscript editions in the methods section. K.B.S contributed with manuscript editions and discussion regarding the hibernating phenotype. F.B funded the study, contributed with the experiment design and contributed with manuscript editions.

Data accessibility statement

The data presented in this paper will be accessible in dryad and raw data from the sequencing runs were deposited at the Sequence Read Archive (SRA) repository of the National Center for Biotechnology Information (NCBI) under accession number SRR6255590- SRR6255614 of the Bioproject PRJNA416414.

Competing interests statement

The authors declare no competing interests

Figure captions

Fig 1. A-C Volcano plots showing differentially regulated genes at the P=0.05 level (green, horizontal line) in three tissues of torpid *D. gliroides* as compared with active animals. Significantly down-regulated genes are indicated as negative fold change (blue), and up-regulated genes are indicated as positive values (red). The gray zone indicates the number of transcripts that do not show significant differential expression. A: brain; B: liver; C: skeletal muscle. D: commonly up-regulated genes among organs (upper panel) and commonly down-regulated genes (bottom panel). The numbers represent the numbers of transcripts that were differentially regulated exclusively for each organ (e.g., 44 transcripts were exclusively and significantly up-regulated in muscle). Most differentially regulated genes are written in yellow and white font on the diagrams. Descriptions of the top 10 significantly regulated genes are provided in Supplementary Tables 2 to 7). Several isoforms of the *TXNIP* gene were found among the upregulated genes in brain, which are denoted by the red ellipse (Fig 1A).

Fig 2. Functional enrichment analysis of genes that appeared over-represented during torpor using the gene ontology database (A). The size of the circles represents the number of differentially expressed genes over the total number of genes, associated to a given GO term; whereas the color indicates the level of significance. Also a functional enrichment analysis using the Kyoto Encyclopedia of Genes and Genomes (KEGG-database) is shown for brain (B), liver (C) and muscle (D). In this analysis, genes are indicated at the left side of each pie graph, with the respective level of expression (Log2 FC) indicated in color in the small squares, and metabolic pathways are indicated in the right side of the graph, connected to the group of genes that are associated to the pathway by lines.

Supplementary Fig 1. Top five overexpressed (top panel) and under-expressed (bottom panel) genes found in the brain of torpid (n=7) and active (n=6) monito del monte expressed in transcripts per million sequences (TPM, mean ± SEM). Gene names and $\log_2$[fold-change] (FC) values are as follows: (A) *TXNIP* = thioredoxin-interacting protein (FC=2.43); (B) *HIST2H2AC* = histone H2A type 2C (FC =2.10); (C) *ANGPTL4* = angiopoietin-related protein 4 (FC = 1.88); (D) *ZNF638* = zinc finger protein 638 (FC = 1.76); (E) *GPR34* = G-protein coupled receptor 34(FC = 1.67); (F) *ATG3* = ubiquitin like-conjugating enzyme ($\log_2$ fold-change= -1.54); (G) *SRSF5* = serine/arginine-rich splicing factor 5 (FC = -1.33); (H) *SF3A1* = splicing factor 3A subunit 1 (FC = -1.30); (I) *TMED3* = transmembrane emp24 domain containing protein 3 (FC = -1.27); (J) *KCNJ13* = inward rectifier potassium channel 13 (FC = -1.24). Fold-change represents the times a transcript was found over-expressed or under-expressed relative to the active control (i.e., a $\log_2$ fold change = 2.85 means $2^{2.85}$ times overexpression; negative fold-changes mean under-expression). More details about these genes and the functions of the proteins that they encode are given in Supplementary Tables 2 to 7.

Supplementary Fig 2. Top five overexpressed (top panel) and under-expressed (bottom panel) genes found in the liver of torpid (n=3) and active (n=3) individuals expressed in

transcripts per million sequences (TPM, mean ± SEM). Gene names and log_2[fold-change] (FC) values are as follows: (A) *GARS* = glycine-tRNA ligase (FC=6.82); (B) *PER3* = period circadian protein homolog 3 (FC =6.46); (C) *PDP2* = pyruvate dehydrogenase phosphatase (mitochondrial) (FC = 6.10); (D) *CYB5R3* = NADH- cytochrome b5 reductase 3 isoform X1 (FC = 6.09); (E) *TXNIP* = thioredoxin-interacting protein (FC=6.03); (F) *TCAF2* = TRPM8 channel-associated factor 2 isoform X2 (FC = -5.97); (G) *NR1H4* = nuclear receptor subfamily 1, group H, member 4 also known as the bile acid receptor (BAR) or the farnesoid X receptor (FXR) (FC = -5.81); (H) *KLHDC3* = kelch domain-containing protein 3 (FC = -5.53); (I) *ND4* = NADH dehydrogenase subunit 4 (mitochondrial) (FC = -5.49); (J) *SLC2A9* = Solute carrier family 2, facilitated glucose transporter member 9 (FC = -5.41). More details about these genes and the functions of the proteins that they encode are given in Supplementary Tables 2 to 7. Some bars are at zero because no transcripts were detected for such gene and condition.

Supplementary Fig 3. Top five overexpressed (top panel) and under-expressed (bottom panel) genes found in skeletal muscle or torpid (n=2) and active (n=2) individuals expressed in transcripts per million sequences (TPM, mean ± SEM). Gene names and log_2[fold-change] (FC) values are as follows: (A) *PVALB* = parvalbumin alpha (FC=7.99); (B) *TXNIP* = thioredoxin-interacting protein (FC=6.09); (C) *DDX17* = ATP-dependent RNA helicase (FC=5.79); (D) *EIF3D* = eukaryotic translation initiation factor 3 subunit D (FC=5.76); (E) *GAPDH* = glyceraldehyde-3-phosphate dehydrogenase (FC=5.65); (F) *ABCB8* = ATP binding cassette subfamily B (mitochondrial)(FC=-5.33); (G) *DDI2* = protein DDI1 homolog 2 (FC=-5.07); (H) *SBF2* = myotubularin-related protein 2 (FC = -4.58); (I) *STXBP2* = syntaxin-binding protein 2 (FC = -4.51); (j) *CEP85* = centrosomal protein of 85 kDa (FC = -4.43). More details about these genes and the functions of the proteins that they encode are given in Supplementary Tables 2 to 7. Some bars at zero because no transcripts were detected for such gene and condition.

Supplementary Fig 4. Expression profiles of each organ, per individual, per treatment ("heatmaps"). Each individual and condition (e.g., Torpor1, Torpor2, Active1, Active2, etc), is indicated at the X-axis. The expression level [an adimensional Z-score based on log(FC)] is indicated by the color (under-expressed genes in blue; overexpressed genes in red). Each gene is indicated as a list, at the right side of each profile (only significantly regulated genes are shown, according to the log(FDR) adjusted values of Fig 1A-C). Lines at the left side of each profile indicate gene clustering according to their expression patterns.

~~***Figure captions***~~

~~Fig 1. A-C Volcano plots showing differentially regulated genes at the P=0.05 level (green, horizontal line) in three tissues of torpid *D. gliroides* as compared with active animals. Significantly down regulated genes are indicated as negative fold change (blue), and up-regulated genes are indicated as positive values (red). The gray zone indicates the number of transcripts that do not show significant differential expression. A: brain; B: liver; C: skeletal muscle. D: commonly up regulated genes among organs (upper panel) and commonly down regulated genes (bottom panel). The numbers represent the numbers of transcripts that were differentially regulated exclusively for each organ (e.g., 44 transcripts~

were exclusively and significantly up regulated in muscle). Most differentially regulated genes are written in yellow and white font on the diagrams. Descriptions of the top 10 significantly regulated genes are provided in Tables A1 to A6 (Supplementary Information). Several isoforms of the *TXNIP* gene were found among the upregulated genes in brain, which are denoted by the red ellipse (Fig 1A).

Fig 2. Top five overexpressed (top panel) and under expressed (bottom panel) genes found in the brain of torpid (n=7) and active (n=6) monito del monte expressed in transcripts per million sequences (TPM, mean ± SEM). Gene names and $\log_2$[fold change] (FC) values are as follows: (A) *TXNIP* = thioredoxin interacting protein (FC=2.43); (B) *HIST2H2AC* = histone H2A type 2C (FC =2.10); (C) *ANGPTL4* = angiopoietin related protein 4 (FC = 1.88); (D) *ZNF638* = zinc finger protein 638 (FC = 1.76); (E) *GPR34* = G protein coupled receptor 34(FC = 1.67); (F) *ATG3* = ubiquitin like conjugating enzyme ($\log_2$ fold change= -1.54); (G) *SRSF5* = serine/arginine rich splicing factor 5 (FC = -1.33); (H) *SF3A1* = splicing factor 3A subunit 1 (FC = -1.30); (I) *TMED3* = transmembrane emp24 domain containing protein 3 (FC = -1.27); (J) *KCNJ13* = inward rectifier potassium channel 13 (FC = -1.24). Fold change represents the times a transcript was found over expressed or under expressed relative to the active control (i.e., a $\log_2$ fold change = 2.85 means $2^{2.85}$ times overexpression; negative fold-changes mean under-expression). More details about these genes and the functions of the proteins that they encode are given in Tables A1 and A2.

Fig 3. Top five overexpressed (top panel) and under expressed (bottom panel) genes found in the liver of torpid (n=3) and active (n=3) individuals expressed in transcripts per million sequences (TPM, mean ± SEM). Gene names and $\log_2$[fold change] (FC) values are as follows: (A) *GARS* = glycine tRNA ligase (FC=6.82); (B) *PER3* = period circadian protein homolog 3 (FC =6.46); (C) *PDP2* = pyruvate dehydrogenase phosphatase (mitochondrial) (FC = 6.10); (D) *CYB5R3* = NADH cytochrome b5 reductase 3 isoform X1 (FC = 6.09); (E) *TXNIP* = thioredoxin interacting protein (FC=6.03); (F) *TCAF2* = TRPM8 channel-associated factor 2 isoform X2 (FC = -5.97); (G) *NR1H4* = nuclear receptor subfamily 1, group H, member 4 also known as the bile acid receptor (BAR) or the farnesoid X receptor (FXR) (FC = -5.81); (H) *KLHDC3* = kelch domain-containing protein 3 (FC = -5.53); (I) *ND4* = NADH dehydrogenase subunit 4 (mitochondrial) (FC = -5.49); (J) *SLC2A9* = Solute carrier family 2, facilitated glucose transporter member 9 (FC = -5.41). More details about these genes and the functions of the proteins that they encode are given in Tables A3 and A4. Some bars are at zero because no transcripts were detected for such gene and condition.

Fig 4. Top five overexpressed (top panel) and under expressed (bottom panel) genes found in skeletal muscle or torpid (n=2) and active (n=2) individuals expressed in transcripts per million sequences (TPM, mean ± SEM). Gene names and $\log_2$[fold change] (FC) values are as follows: (A) *PVALB* = parvalbumin alpha (FC=7.99); (B) *TXNIP* = thioredoxin-interacting protein (FC=6.09); (C) *DDX17* = ATP dependent RNA helicase (FC=5.79); (D) *EIF3D* = eukaryotic translation initiation factor 3 subunit D (FC=5.76); (E) *GAPDH* = glyceraldehyde 3 phosphate dehydrogenase (FC=5.65); (F) *ABCB8* = ATP binding cassette subfamily B (mitochondrial)(FC= 5.33); (G) *DDI2* = protein DDI1 homolog 2 (FC= 5.07); (H) *SBF2* = myotubularin related protein 2 (FC = -4.58); (I) *STXBP2* = syntaxin binding protein 2 (FC = -4.51); (j) *CEP85* = centrosomal protein of 85 kDa (FC = -4.43). More

~~details about these genes and the functions of the proteins that they encode are given in Tables A5 and A6. Some bars at zero because no transcripts were detected for such gene and condition.~~

~~Fig 5. Functional enrichment analysis of genes that appeared over represented during torpor using the gene ontology database (A). The size of the circles represents the number of differentially expressed genes over the total number of genes, associated to a given GO term; whereas the color indicates the level of significance. Also a functional enrichment analysis using the Kyoto Encyclopedia of Genes and Genomes (KEGG database) is shown for brain (B), liver (C) and muscle (D). In this analysis, genes are indicated at the left side of each pie graph, with the respective level of expression (LogFC) indicated in color in the small squares, and metabolic pathways are indicated in the right side of the graph, connected to the group of genes that are associated to the pathway by lines.~~

~~Fig A1. Expression profiles of each organ, per individual, per treatment ("heatmaps"). Each individual and condition (e.g., Torpor1, Torpor2, Active1, Active2, etc), is indicated at the X axis. The expression level [an adimensional Z score based on log(FC)] is indicated by the color (under-expressed genes in blue; overexpressed genes in red). Each gene is indicated as a list, at the right side of each profile (only significantly regulated genes are shown, according to the log(FDR) adjusted values of Fig 1A-C). Lines at the left side of each profile indicate gene clustering according to their expression patterns.~~

References

Altschul, S. F., Gish, W., Miller, W., Myers, E. W., & Lipman, D. J. (1990). BASIC LOCAL ALIGNMENT SEARCH TOOL. *Journal of molecular biology, 215*(3), 403-410. doi:10.1006/jmbi.1990.9999

Andres-Mateos, E., Mejias, R., Soleimani, A., Lin, B. M., Burks, T. N., Marx, R., . . . Cohn, R. D. (2012). Impaired skeletal muscle regeneration in the absence of fibrosis during hibernation in 13-lined ground squirrels. *Plos One, 7*(11), e48884. doi:e48884

10.1371/journal.pone.0048884

Andrews, M. T. (2004). Genes controlling the metabolic switch in hibernating mammals. *Biochemical Society Transactions, 32*, 1021-1024.

Ashburner, M., Ball, C. A., Blake, J. A., Botstein, D., Butler, H., Cherry, J. M., . . . Gene Ontology, C. (2000). Gene Ontology: tool for the unification of biology. *Nature Genetics, 25*(1), 25-29.

Babicki, S., Arndt, D., Marcu, A., Liang, Y. J., Grant, J. R., Maciejewski, A., & Wishart, D. S. (2016). Heatmapper: web-enabled heat mapping for all. *Nucleic Acids Research, 44*(W1), W147-W153. doi:10.1093/nar/gkw419

Bogacka, I., Paukszto, T., Jastrzebski, J. P., Czerwinska, J., Chojnowska, K., Kaminska, B., . . . Kaminski, T. (2017). Seasonal differences in the testicular transcriptome profile of free-living European beavers (Castor fiber L.) determined by the RNA-Seq method. *Plos One, 12*(7), 20. doi:10.1371/journal.pone.0180323

816 Bolger, A. M., Lohse, M., & Usadel, B. (2014). Trimmomatic: a flexible trimmer for
817 Illumina sequence data. *Bioinformatics, 30*(15), 2114-2120.
818 doi:10.1093/bioinformatics/btu170
819 Boyer, B. B., & Barnes, B. M. (1999). Molecular and metabolic aspects of mammalian
820 hibernation. *Bioscience, 49*, 713-724.
821 Boyles, J. G., Thompson, A. B., McKechnie, A. E., Malan, E., Humphries, M. M., & Careau,
822 V. (2013). A global heterothermic continuum in mammals. *Global Ecology and*
823 *Biogeography, 22*(9), 1029-1039. doi:10.1111/geb.12077
824 Bozinovic, F., Ruiz, G., & Rosenmann, M. (2004). Energetics and torpor of a South
825 American "living fossil", the Microbiotheriid *Dromiciops gliroides*. *Journal of*
826 *Comparative Physiology B, 174*, 293-297.
827 Carey, H. V., Andrews, M. T., & Martin, S. L. (2003). Mammalian hibernation: Cellular
828 and molecular responses to depressed metabolism and low temperature.
829 *Physiological Reviews, 83*(4), 1153-1181. doi:10.1152/physrev.00008.2003
830 Cariou, B., Bouchaert, E., Abdelkarim, M., Dumont, J., Caron, S., Fruchart, J. C., . . . Staels,
831 B. (2007). FXR-deficiency confers increased susceptibility to torpor. *FEBS*
832 *letters, 581*(27), 5191-5198. doi:10.1016/j.febslet.2007.09.064
833 Chong, C. R., Chan, W. P. A., Nguyen, T. H., Liu, S. F., Procter, N. E. K., Ngo, D. T., . . .
834 Horowitz, J. D. (2014). Thioredoxin-Interacting Protein: Pathophysiology and
835 Emerging Pharmacotherapeutics in Cardiovascular Disease and Diabetes.
836 *Cardiovascular Drugs and Therapy, 28*(4), 347-360. doi:10.1007/s10557-014-
837 6538-5
838 Conesa, A., Gotz, S., Garcia-Gomez, J. M., Terol, J., Talon, M., & Robles, M. (2005).
839 Blast2GO: a universal tool for annotation, visualization and analysis in
840 functional genomics research. *Bioinformatics, 21*(18), 3674-3676.
841 doi:10.1093/bioinformatics/bti610
842 Contreras, C., Franco, M., Place, N. J., & Nespolo, R. F. (2014). The effects of poly-
843 unsaturated fatty acids on the physiology of hibernation in a South American
844 marsupial, Dromiciops gliroides. *Comparative Biochemistry and Physiology a-*
845 *Molecular & Integrative Physiology, 177*, 62-69. doi:10.1016/j.cbpa.2014.07.004
846 Cooper, S. T., Sell, S. S., Fahrenkrog, M., Wilkinson, K., Howard, D. R., Bergen, H., . . .
847 Hampton, M. (2016). Effects of hibernation on bone marrow transcriptome in
848 thirteen-lined ground squirrels. *Physiological Genomics, 48*(7), 513-525.
849 doi:10.1152/physiolgenomics.00120.2015
850 Crawford, F. I. J., Hodgkinson, C. L., Ivanova, E., Logunova, L. B., Evans, G. J.,
851 Steinlechner, S., & Loudon, A. S. I. (2007). Influence of torpor on cardiac
852 expression of genes involved in the circadian clock and protein turnover in the
853 Siberian hamster (Phodopus sungorus). *Physiological Genomics, 31*(3), 521-
854 530. doi:10.1152/physiolgenomics.00131.2007
855 De Wit, P., Pespeni, M. H., Ladner, J. T., Barshis, D. J., Seneca, F., Jaris, H., . . . Palumbi, S.
856 R. (2012). The simple fool's guide to population genomics via RNA-Seq: an
857 introduction to high-throughput sequencing data analysis. *Molecular Ecology*
858 *Resources, 12*(6), 1058-1067. doi:10.1111/1755-0998.12003
859 DeBalsi, K. L., Wong, K. E., Koves, T. R., Slentz, D. H., Seiler, S. E., Wittmann, A. H., . . .
860 Lark, D. S. (2014). Targeted metabolomics connects thioredoxin-interacting
861 protein (TXNIP) to mitochondrial fuel selection and regulation of specific

oxidoreductase enzymes in skeletal muscle. *Journal of Biological Chemistry, 289*(12), 8106-8120.

Eddy, S. F., Morin, P. J. R., & Storey, K. B. (2006). Differential expression of selected mitochondrial genes in hibernating little brown bats, Myotis lucifiugus. *Journal of Experimental Zoology Part a-Comparative Experimental Biology, 305A*(8), 620-630. doi:10.1002/jez.a.294

Eshbach, M. L., Sethi, R., Avula, R., Lamb, J., Hollingshead, D. J., Finegold, D. N., . . . Weisz, O. A. (2017). The transcriptome of the Didelphis virginiana opossum kidney OK proximal tubule cell line. *American Journal of Physiology-Renal Physiology, 313*(3), F585-F595. doi:10.1152/ajprenal.00228.2017

Faherty, S. L., Villanueva-Canas, J. L., Klopfer, P. H., Alba, M. M., & Yoder, A. D. (2016). Gene Expression Profiling in the Hibernating Primate, Cheirogaleus Medius. *Genome Biology and Evolution, 8*(8), 2413-2426. doi:10.1093/gbe/evw163

Fahlman, A., Storey, J. M., & Storey, K. B. (2000). Gene up-regulation in heart during mammalian hibernation. *Cryobiology, 40*(4), 332-342. doi:10.1006/cryo.2000.2254

Fedorov, V. B., Goropashnaya, A. V., Stewart, N. C., Toien, O., Chang, C., Wang, H. F., . . . Barnes, B. M. (2014). Comparative functional genomics of adaptation to muscular disuse in hibernating mammals. *Molecular Ecology, 23*(22), 5524-5537. doi:10.1111/mec.12963

Ferreira, J. A., & Zwinderman, A. H. (2006). On the Benjamini-Hochberg method. *Annals of Statistics, 34*(4), 1827-1849. doi:10.1214/009053606000000425

Fons, R., Sender, S., Peters, T., & Jurgens, K. D. (1997). Rates of rewarming, heart andrespiratory rates and their significance for oxygen transport during arousal from torpor in the smallest mammal, the etruscan shrew *Suncus etruscus*. *Journal of Experimental Biology, 200*, 1451-1458.

Franco, M., Contreras, C., & Nespolo, R. F. (2013). Profound changes in blood parameters during torpor in a South American marsupial. *Comparative Biochemistry and Physiology a-Molecular & Integrative Physiology, 166*(2), 338-342. doi:10.1016/j.cbpa.2013.07.010

Franco, M., Contreras, C., Place, N. J., Bozinovic, F., & Nespolo, R. F. (2017). Leptin levels, seasonality and thermal acclimation in the Microbiotherid marsupial Dromiciops gliroides: Does photoperiod play a role? *Comparative Biochemistry and Physiology a-Molecular & Integrative Physiology, 203*, 233-240. doi:10.1016/j.cbpa.2016.09.025

Gannon, W. L., Sikes, R. S., & Comm, A. C. U. (2007). Guidelines of the American Society of Mammalogists for the use of wild mammals in research. *Journal of Mammalogy, 88*(3), 809-823. doi:10.1644/06-mamm-f-185r1.1

Garcia-Martinez, J. M., & Alessi, D. R. (2008). mTOR complex 2 (mTORC2) controls hydrophobic motif phosphorylation and activation of serum- and glucocorticoid-induced protein kinase 1 (SGK1). *Biochemical Journal, 416*, 375-385. doi:10.1042/bj20081668

Geiser, F., & Martin, G. M. (2013). Torpor in the Patagonian opossum (Lestodelphys halli): implications for the evolution of daily torpor and hibernation. *Naturwissenschaften, 100*(10), 975-981. doi:10.1007/s00114-013-1098-2

907 Grabherr, M. G., Haas, B. J., Yassour, M., Levin, J. Z., Thompson, D. A., Amit, I., . . . Regev,
908 A. (2011). Full-length transcriptome assembly from RNA-Seq data without a
909 reference genome. *Nature Biotechnology, 29*(7), 644-U130.
910 doi:10.1038/nbt.1883
911 Graves, J. A. M., & Renfree, M. B. (2013). Marsupials in the Age of Genomics. In A.
912 Chakravarti & E. Green (Eds.), *Annual Review of Genomics and Human Genetics,*
913 *Vol 14* (Vol. 14, pp. 393-420). Palo Alto: Annual Reviews.
914 Gurevich, A., Saveliev, V., Vyahhi, N., & Tesler, G. (2013). QUAST: quality assessment
915 tool for genome assemblies. *Bioinformatics, 29*(8), 1072-1075.
916 doi:10.1093/bioinformatics/btt086
917 Habel, J. C., Assman, T., Schmidtt, T., & Avise, J. C. (2010). Relict species: from past to
918 future. In J. C. Habel & T. Assman (Eds.), *Relict Species. Phylogeography and*
919 *Conservation Biology*. Berlin: Springer.
920 Hadj-Moussa, H., Moggridge, J. A., Luu, B. E., Quiuntero-Galvis, J. F., Gaitan-Espitia, J. D.,
921 Nespolo, R. F., & Storey, K. B. (2016). The hibernating South American
922 marsupial, Dromiciops gliroides, display torpor-sensititve microRNA
923 expression patterns. *Scientific Reports*. doi:DOI: 10.1038/srep24627
924 Hand, L. E., Saer, B. R. C., Hui, S. T., Jinnah, H. A., Steinlechner, S., Loudon, A. S. I., &
925 Bechtold, D. A. (2013). Induction of the Metabolic Regulator Txnip in Fasting-
926 Induced and Natural Torpor. *Endocrinology, 154*(6), 2081-2091.
927 doi:10.1210/en.2012-2051
928 Harris, R. A., Bowker-Kinley, M. M., Huang, B. L., & Wu, P. F. (2002). Regulation of the
929 activity of the pyruvate dehydrogenase complex. In G. Weber (Ed.), *Advances in*
930 *Enzyme Regulation, Vol 42, Proceedings* (Vol. 42, pp. 249-259). Oxford:
931 Pergamon-Elsevier Science Ltd.
932 Hershkovitz, P. (1999). Dromiciops gliroides Thomas, 1894, Last of the Microbiotheria
933 (Marsupialia), with a review of the family Microbiotheridae. *Fieldana, 93*, 1-60.
934 Hindle, A. G., Karimpour-Fard, A., Epperson, L. E., Hunter, L. E., & Martin, S. L. (2011).
935 Skeletal muscle proteomics: carbohydrate metabolism oscillates with seasonal
936 and torpor-arousal physiology of hibernation. *American Journal of Physiology-*
937 *Regulatory Integrative and Comparative Physiology, 301*(5), R1440-R1452.
938 doi:10.1152/ajpregu.00298.2011
939 Il'ina, T. N., Ilyukha, V. A., Baishnikova, I. V., Belkin, V. V., Sergina, S. N., & Antonova, E.
940 P. (2017). Antioxidant defense system in tissues of semiaquatic mammals.
941 *Journal of Evolutionary Biochemistry and Physiology, 53*(4), 282-288.
942 doi:10.1134/s0022093017040044
943 Jastroch, M., Giroud, S., Barrett, P., Geiser, F., Heldmaier, G., & Herwig, A. (2016).
944 Seasonal Control of Mammalian Energy Balance: Recent Advances in the
945 Understanding of Daily Torpor and Hibernation. *Journal of Neuroendocrinology,*
946 *28*(11), 10. doi:10.1111/jne.12437
947 Jastroch, M., Wuertz, S., Kloas, W., & Klingenspor, M. (2005). Uncoupling protein 1 in
948 fish uncovers an ancient evolutionary history of mammalian nonshivering
949 thermogenesis. *Physiological Genomics, 22*(2), 150-156.
950 doi:10.1152/physiolgenomics.00070.2005

951 Jiao, Y., Lu, Y., & Li, X. Y. (2015). Farnesoid X receptor: a master regulator of hepatic
952 triglyceride and glucose homeostasis. *Acta Pharmacologica Sinica, 36*(1), 44-50.
953 doi:10.1038/aps.2014.116
954 Jones, P., Binns, D., Chang, H. Y., Fraser, M., Li, W. Z., McAnulla, C., . . . Hunter, S. (2014).
955 InterProScan 5: genome-scale protein function classification. *Bioinformatics,*
956 *30*(9), 1236-1240. doi:10.1093/bioinformatics/btu031
957 Koteja, P. (2004). The evolution of concepts on the evolution of endothermy in birds
958 and mammals. *Physiological and Biochemical Zoology, 77*, 1043-1050.
959 Krzywinski, M., Schein, J., Birol, I., Connors, J., Gascoyne, R., Horsman, D., . . . Marra, M.
960 A. (2009). Circos: An information aesthetic for comparative genomics. *Genome*
961 *Research, 19*(9), 1639-1645. doi:10.1101/gr.092759.109
962 Langmead, B., & Salzberg, S. L. (2012). Fast gapped-read alignment with Bowtie 2.
963 *Nature Methods, 9*(4), 357-U354. doi:10.1038/nmeth.1923
964 Li, B., & Dewey, C. N. (2011). RSEM: accurate transcript quantification from RNA-Seq
965 data with or without a reference genome. *Bmc Bioinformatics, 12*, 16.
966 doi:10.1186/1471-2105-12-323
967 Liu, M. M., Farkas, M., Spinnhirny, P., Pevet, P., Pierce, E., Hicks, D., & Zack, D. J. (2017).
968 De novo assembly and annotation of the retinal transcriptome for the Nile
969 grass rat (Arvicanthis ansorgei). *Plos One, 12*(7), 14.
970 doi:10.1371/journal.pone.0179061
971 Love, M. I., Huber, W., & Anders, S. (2014). Moderated estimation of fold change and
972 dispersion for RNA-seq data with DESeq2. *Genome Biology, 15*(12), 38.
973 doi:10.1186/s13059-014-0550-8
974 Luu, B. E., Wijenayake, S., Zhang, J., Tessier, S. N., Quintero-Galvis, J. F., Gaitan-Espitia, J.
975 D., . . . Storey, J. M. (2018a). Strategies of biochemical adaptation for
976 hibernation in a south American marsupial, Dromiciops gliroides: 2. Control of
977 the Akt pathway and protein translation machinery. *Comparative Biochemical*
978 *Physiology B*.
979 Luu, B. E., Wijenayake, S., Zhang, J., Tessier, S. N., Quintero-Galvis, J. F., Gaitan-Espitia, J.
980 D., . . . Storey, K. B. (2018b). Strategies of biochemical adaptation for
981 hibernation in a south American marsupial, Dromiciops gliroides: 3. Activation
982 of pro-survival response pathways. *Comparative Biochemical Physiology B*.
983 Malan, A. (2010). Is the Torpor-Arousal Cycle of Hibernation Controlled by a Non-
984 Temperature-Compensated Circadian Clock? *Journal of Biological Rhythms,*
985 *25*(3), 166-175. doi:10.1177/0748730410368621
986 Maulik, N., & Das, D. K. (2008). Emerging potential of thioredoxin and thioredoxin
987 interacting proteins in various disease conditions. *Biochimica Et Biophysica*
988 *Acta-General Subjects, 1780*(11), 1368-1382.
989 doi:10.1016/j.bbagen.2007.12.008
990 Mitchell, K. J., Pratt, R. C., Watson, L. N., Gibb, G. C., Llamas, B., Kasper, M., . . . Cooper, A.
991 (2014). Molecular Phylogeny, Biogeography, and Habitat Preference Evolution
992 of Marsupials. *Molecular Biology and Evolution, 31*(9), 2322-2330.
993 doi:10.1093/molbev/msu176
994 Morin, P., & Storey, K. B. (2009). Mammalian hibernation: differential gene expression
995 and novel application of epigenetic controls. *International Journal of*
996 *Developmental Biology, 53*(2-3), 433-442. doi:10.1387/ijdb.082643pm

997 Moriya, Y., Itoh, M., Okuda, S., Yoshizawa, A. C., & Kanehisa, M. (2007). KAAS: an
998 automatic genome annotation and pathway reconstruction server. *Nucleic*
999 *Acids Research, 35*, W182-W185. doi:10.1093/nar/gkm321
1000 Morris, K. M., Weaver, H. J., O'Meally, D., Desclozeaux, M., Gillett, A., & Polkinghorne, A.
1001 (2018). Transcriptome sequencing of the long-nosed bandicoot (Perameles
1002 nasuta) reveals conservation and innovation of immune genes in the marsupial
1003 order Peramelemorphia. *Immunogenetics, 70*(5), 327-336.
1004 doi:10.1007/s00251-017-1043-1
1005 Nelson, C. J., Otis, J. P., & Carey, H. V. (2009). A role for nuclear receptors in mammalian
1006 hibernation. *Journal of Physiology-London, 587*(9), 1863-1870.
1007 doi:10.1113/jphysiol.2008.167692
1008 Nespolo, R. F., Bacigalupe, L. D., Figueroa, C. C., Koteja, P., & Opazo, J. C. (2011). Using
1009 new tools to solve an old problem: the evolution of endothermy in vertebrates.
1010 *Trends in Ecology & Evolution, 26*(8), 414-423. doi:10.1016/j.tree.2011.04.004
1011 Nespolo, R. F., Verdugo, C., Cortes, P. A., & Bacigalupe, L. D. (2010). Bioenergetics of
1012 torpor in the Microbiotherid marsupial, Monito del Monte (*Dromiciops*
1013 *gliroides*): the role of temperature and food availability. *Journal of Comparative*
1014 *Physiology B-Biochemical Systemic and Environmental Physiology, 180*(5), 767-
1015 773. doi:10.1007/s00360-010-0449-y
1016 Nishiyama, A., Matsui, M., Iwata, S., Hirota, K., Masutani, H., Nakamura, H., . . . Yodoi, J.
1017 (1999). Identification of thioredoxin-binding protein-2/vitamin D-3 up-
1018 regulated protein 1 as a negative regulator of thioredoxin function and
1019 expression. *Journal of Biological Chemistry, 274*(31), 21645-21650.
1020 doi:10.1074/jbc.274.31.21645
1021 Opazo, J. C., Nespolo, R. F., & Bozinovic, F. (1999). Arousal from torpor in the chilean
1022 mouse-opposum (*Thylamys elegans*): does non-shivering thermogenesis play a
1023 role? *Comparative Biochemistry and Physiology A, 123*, 393-397.
1024 Palma, R. E., & Spotorno, A. E. (1999). Molecular systematics of marsupials based on
1025 the rRNA 12S mitochondrial gene: The phylogeny of didelphimorphia and of
1026 the living fossil microbiotheriid Dromiciops gliroides Thomas. *Molecular*
1027 *Phylogenetics and Evolution, 13*(3), 525-535. doi:10.1006/mpev.1999.0678
1028 Platani, M., Samejima, I., Samejima, K., Kanemaki, M. T., & Earnshaw, W. C. (2018).
1029 Seh1 targets GATOR2 and Nup153 to mitotic chromosomes. *Journal of Cell*
1030 *Science, 131*. doi:10.1242/jcs.213140
1031 Renfree, M. B. (1981). Marsupials: alternative mammals. *Nature, 293*, 100-101.
1032 Rose, J. C., Epperson, L. E., Carey, H. V., & Martin, S. L. (2011). Seasonal liver protein
1033 differences in a hibernator revealed by quantitative proteomics using whole
1034 animal isotopic labeling. *Comparative Biochemistry and Physiology D-Genomics*
1035 *& Proteomics, 6*(2), 163-170. doi:10.1016/j.cbd.2011.02.003
1036 Rose, R. W., West, A. K., Ye, J. M., McCormack, G. H., & Colquhoun, E. Q. (1999).
1037 Nonshivering thermogenesis in a marsupial (the Tasmanian bettong Bettongia
1038 gaimardi) is not attributable to brown adipose tissue. *Physiological and*
1039 *Biochemical Zoology, 72*(6), 699-704. doi:10.1086/316709
1040 Rouble, A. N., & Storey, K. B. (2015). Characterization of the SIRT family of NAW-
1041 dependent protein deacetylases in the context of a mammalian model of

hibernation, the thirteen-lined ground squirrel. *Cryobiology, 71*(2), 334-343. doi:10.1016/j.cryobiol.2015.08.009

Rouble, A. N., Tessier, S. N., & Storey, K. B. (2014). Characterization of adipocyte stress response pathways during hibernation in thirteen-lined ground squirrels. *Molecular and Cellular Biochemistry, 393*(1-2), 271-282. doi:10.1007/s11010-014-2070-y

Ruf, T., & Geiser, F. (2015). Daily torpor and hibernation in birds and mammals. *Biological Reviews, 90*(3), 891-926. doi:10.1111/brv.12137

Schwartz, C., Hampton, M., & Andrews, M. T. (2013). Seasonal and Regional Differences in Gene Expression in the Brain of a Hibernating Mammal. *Plos One, 8*(3). doi:e58427

10.1371/journal.pone.0058427

Simao, F. A., Waterhouse, R. M., Ioannidis, P., Kriventseva, E. V., & Zdobnov, E. M. (2015). BUSCO: assessing genome assembly and annotation completeness with single-copy orthologs. *Bioinformatics, 31*(19), 3210-3212. doi:10.1093/bioinformatics/btv351

Spindel, O. N., World, C., & Berk, B. C. (2012). Thioredoxin Interacting Protein: Redox Dependent and Independent Regulatory Mechanisms. *Antioxidants & Redox Signaling, 16*(6), 587-596. doi:10.1089/ars.2011.4137

Storey, K. B., & Storey, J. M. (2010). METABOLIC RATE DEPRESSION: THE BIOCHEMISTRY OF MAMMALIAN HIBERNATION. In G. S. Makowski (Ed.), *Advances on Clinical Chemistry, Vol 52* (Vol. 52, pp. 77-108).

Travisano, M., & Shaw, R. G. (2013). LOST IN THE MAP. *Evolution, 67*(2), 305-314. doi:10.1111/j.1558-5646.2012.01802.x

Turner, J. M., Warnecke, L., Kortner, G., & Geiser, F. (2012). Opportunistic hibernation by a free-ranging marsupial. *Journal of Zoology, 286*(4), 277-284. doi:10.1111/j.1469-7998.2011.00877.x

van Breukelen, F., Krumschnabel, G., & Podrabsky, J. E. (2010). Vertebrate cell death in energy-limited conditions and how to avoid it: what we might learn from mammalian hibernators and other stress-tolerant vertebrates. *Apoptosis, 15*(3), 386-399. doi:10.1007/s10495-010-0467-y

van Breukelen, F., & Martin, S. L. (2015). The Hibernation Continuum: Physiological and Molecular Aspects of Metabolic Plasticity in Mammals. *Physiology, 30*(4), 273-281. doi:10.1152/physiol.00010.2015

Vermillion, K. L., Anderson, K. J., Hampton, M., & Andrews, M. T. (2015). Gene expression changes controlling distinct adaptations in the heart and skeletal muscle of a hibernating mammal. *Physiological Genomics, 47*(3), 58-74. doi:10.1152/physiolgenomics.00108.2014

Villanueva-Canas, J. L., Faherty, S. L., Yoder, A. D., & Alba, M. M. (2014). Comparative Genomics of Mammalian Hibernators Using Gene Networks. *Integrative and Comparative Biology, 54*(3), 452-462. doi:10.1093/icb/icu048

Villarin, J. J., Schaeffer, P. J., Markle, R. A., & Lindstedt, S. L. (2003). Chronic cold exposure increases liver oxidative capacity in the marsupial Monodelphis domestica *Comparative Biochemistry and Physiology a-Molecular & Integrative Physiology, 136*(3), 621-630.

Wijenayake, S., Luu, B. E., Zhang, J., Tessier, S. N., Quintero-Galvis, J. F., Gaitan-Espitia, J. D., . . . Storey, K. B. (2018a). Strategies of biochemical adaptation for hibernation in a south American marsupial Dromiciops gliroides: 1. Mitogen-activated protein kinases and the cell stress response. *Comparative Biochemical Physiology B*.

Wijenayake, S., Luu, B. E., Zhang, J., Tessier, S. N., Quintero-Galvis, J. F., Gaitan-Espitia, J. D., . . . Storey, K. B. (2018b). Strategies of biochemical adaptation for hibernation in a South American marsupial, Dromiciops gliroides: 4. Regulation of pyruvate dehydrogenase complex and metabolic fuel selection. *Comparative Biochemical Physiology B*.

Wijenayake, S., Tessier, S. N., & Storey, K. B. (2017). Regulation of pyruvate dehydrogenase (PDH) in the hibernating ground squirrel, (Ictidomys tridecemlineatus). *Journal of Thermal Biology, 69*, 199-205. doi:10.1016/j.jtherbio.2017.07.010

Williams, C. R., Baccarella, A., Parrish, J. Z., & Kim, C. C. (2016). Trimming of sequence reads alters RNA-Seq gene expression estimates. *Bmc Bioinformatics, 17*, 13. doi:10.1186/s12859-016-0956-2

Wollam, J., & Antebi, A. (2011). Sterol Regulation of Metabolism, Homeostasis, and Development. In R. D. Kornberg, C. R. H. Raetz, J. E. Rothman, & J. W. Thorner (Eds.), *Annual Review of Biochemistry, Vol 80* (Vol. 80, pp. 885-916). Palo Alto: Annual Reviews.

Yoshioka, J., & Lee, R. T. (2014). Thioredoxin-interacting protein and myocardial mitochondrial function in ischemia-reperfusion injury. *Trends in Cardiovascular Medicine, 24*(2), 75-80. doi:10.1016/j.tcm.2013.06.007

Young, M. D., Wakefield, M. J., Smyth, G. K., & Oshlack, A. (2010). Gene ontology analysis for RNA-seq: accounting for selection bias. *Genome Biology, 11*(2), 12. doi:10.1186/gb-2010-11-2-r14

Zietak, M., Chabowska-Kita, A., & Kozak, L. P. (2017). Brown fat thermogenesis: Stability of developmental programming and transient effects of temperature and gut microbiota in adults. *Biochimie, 134*, 93-98. doi:10.1016/j.biochi.2016.12.006

Formatted: Justified

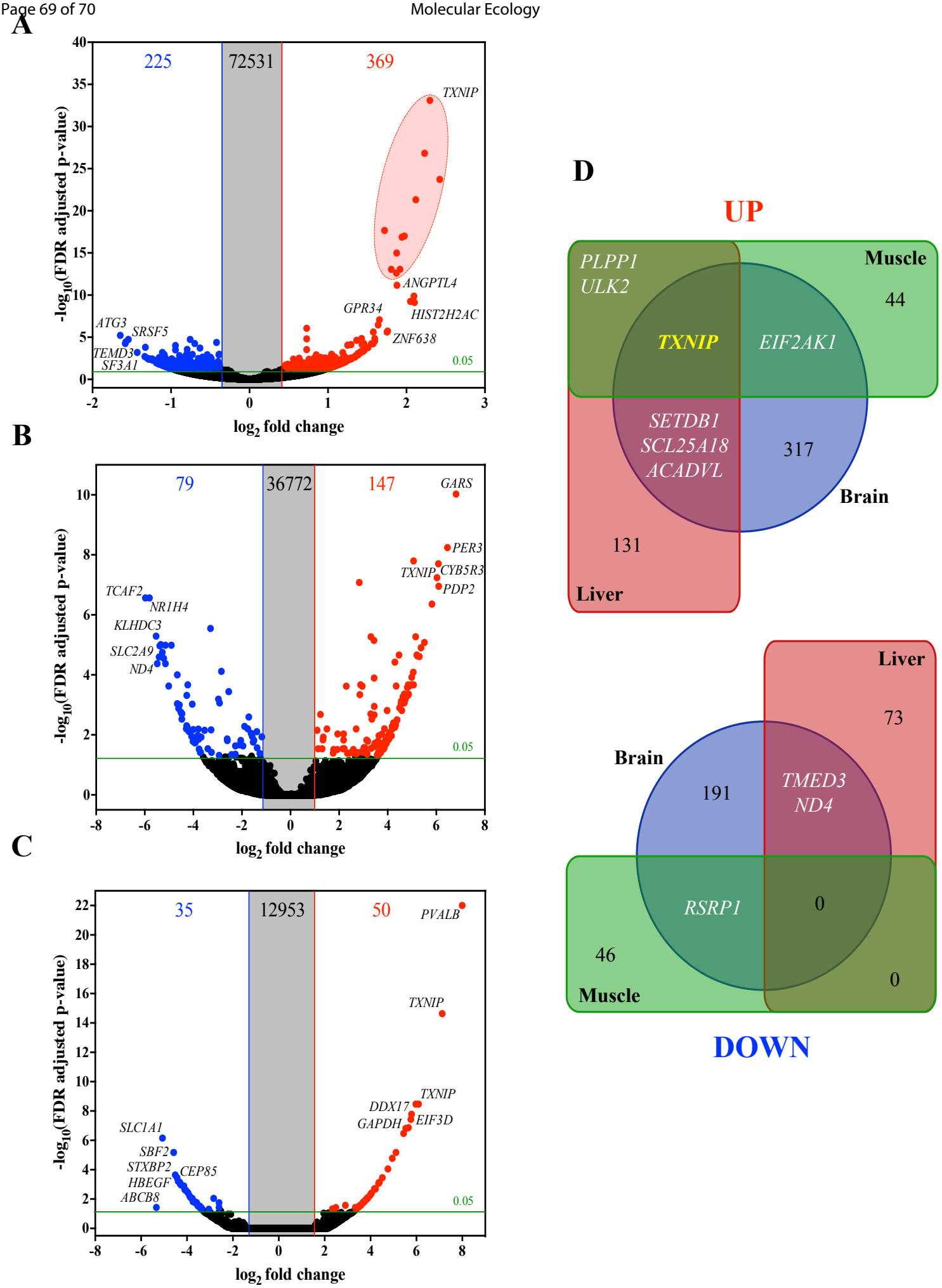
A
225
72531
369
TXNIP
ANGPTL4
GPR34
HIST2H2AC
ZNF638
ATG3
SRSF5
TEMD3
SF3A1
0.05
-log10(FDR adjusted p-value)
log2 fold change
B
79
36772
147
GARS
PER3
TXNIP
CYB5R3
PDP2
TCAF2
NR1H4
KLHDC3
SLC2A9
ND4
0.05
-log10(FDR adjusted p-value)
log2 fold change
C
35
12953
50
PVALB
TXNIP
TXNIP
DDX17
EIF3D
GAPDH
SLC1A1
SBF2
STXBP2
CEP85
HBEGF
ABCB8
0.05
-log10(FDR adjusted p-value)
log2 fold change
D
UP
PLPP1
ULK2
Muscle
44
TXNIP
EIF2AK1
SETDB1
SCL25A18
ACADVL
317
Brain
131
Liver
Liver
73
Brain
191
TMED3
ND4
RSRP1
0
46
0
Muscle
DOWN

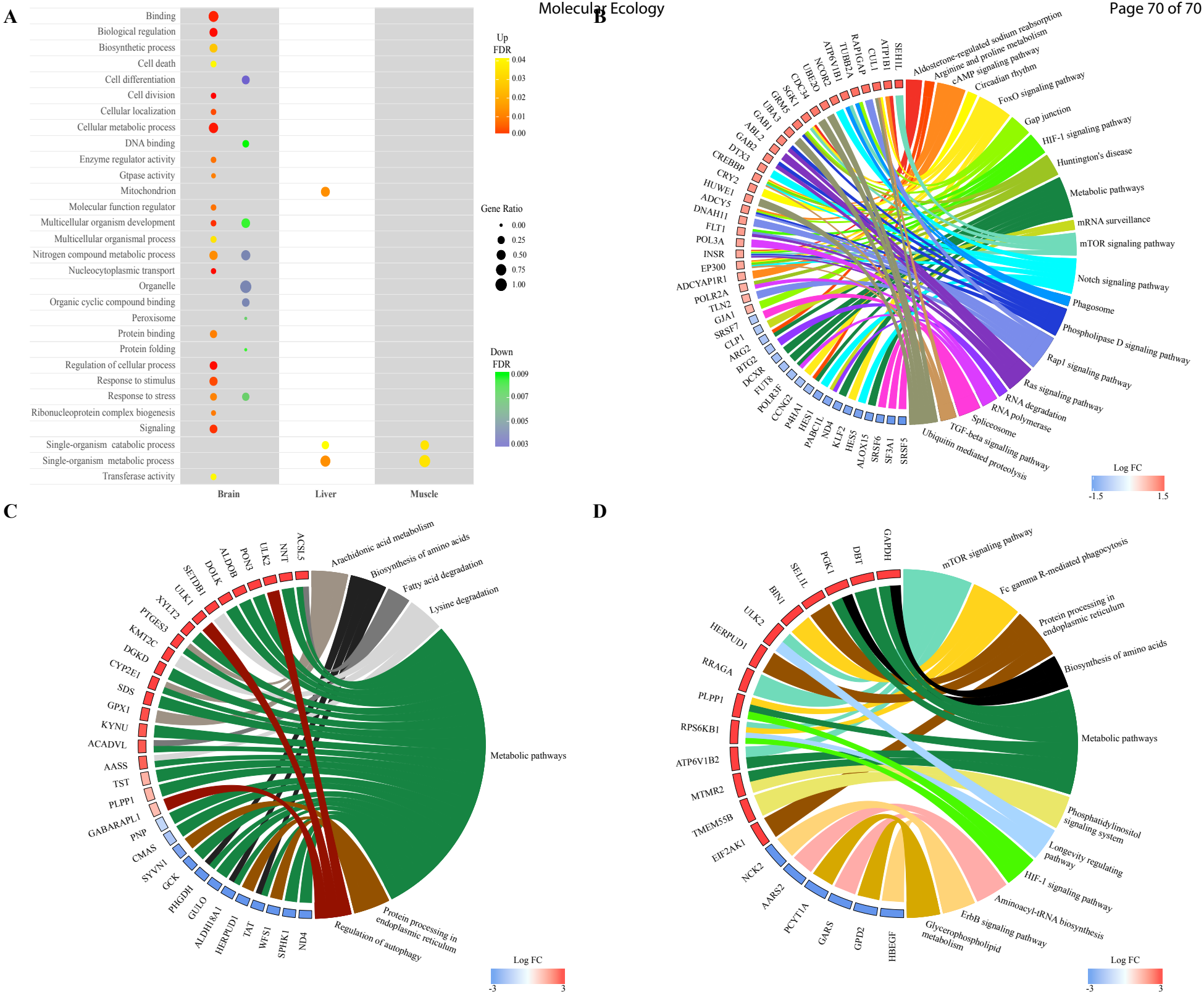
A
Binding
Biological regulation
Biosynthetic process
Cell death
Cell differentiation
Cell division
Cellular localization
Cellular metabolic process
DNA binding
Enzyme regulator activity
Gtpase activity
Mitochondrion
Molecular function regulator
Multicellular organism development
Multicellular organismal process
Nitrogen compound metabolic process
Nucleocytoplasmic transport
Organelle
Organic cyclic compound binding
Peroxisome
Protein binding
Protein folding
Regulation of cellular process
Response to stimulus
Response to stress
Ribonucleoprotein complex biogenesis
Signaling
Single-organism catabolic process
Single-organism metabolic process
Transferase activity
Brain
Liver
Muscle
Up FDR
0.04
0.03
0.02
0.01
0.00
Gene Ratio
0.00
0.25
0.50
0.75
1.00
Down FDR
0.009
0.007
0.005
0.003
B
Aldosterone-regulated sodium reabsorption
Arginine and proline metabolism
cAMP signaling pathway
Circadian rhythm
FoxO signaling pathway
Gap junction
HIF-1 signaling pathway
Huntington's disease
Metabolic pathways
mRNA surveillance
mTOR signaling pathway
Notch signaling pathway
Phagosome
Phospholipase D signaling pathway
Rap1 signaling pathway
Ras signaling pathway
RNA degradation
RNA polymerase
Spliceosome
TGF-beta signalling pathway
Ubiquitin mediated proteolysis
SEH1L
ATP1B1
CUL1
RAP1GAP
TUBB2A
ATP6V1B1
NCOR2
UBE2D
CDC34
SGK1
GRM5
UBA3
GAB1
ABL2
GAB2
DTX3
CREBBP
CRY2
HUWE1
ADCY5
DNAH11
FLT1
POL3A
INSR
EP300
ADCYAP1R1
POLR2A
TLN2
GJA1
SRSF7
CLP1
ARG2
BTG2
DCXR
FUT8
POLR3F
CCNG2
P4HA1
HES1
PABPC1L
ND4
KLF2
HES5
ALOX15
SRSF6
SF3A1
SRSF5
Log FC
-1.5
1.5
C
Arachidonic acid metabolism
Biosynthesis of amino acids
Fatty acid degradation
Lysine degradation
Metabolic pathways
Protein processing in endoplasmic reticulum
Regulation of autophagy
ACSL5
NNT
ULK2
PON3
ALDOB
DOLK
SETDB1
ULK1
XYLT2
PTGES3
KMT2C
DGKD
CYP2E1
SDS
GPX1
KYNU
ACADVL
AASS
TST
PLPP1
GABARAPL1
PNP
CMAS
SYVN1
GCK
PHGDH
GULO
ALDH18A1
HERPUD1
TAT
WFS1
SPHK1
ND4
Log FC
-3
3
D
mTOR signaling pathway
Fc gamma R-mediated phagocytosis
Protein processing in endoplasmic reticulum
Biosynthesis of amino acids
Metabolic pathways
Phosphatidylinositol signaling system
Longevity regulating pathway
HIF-1 signaling pathway
Aminoacyl-tRNA biosynthesis
ErbB signaling pathway
Glycerophospholipid metabolism
GAPDH
DBT
PGK1
SEL1L
BIN1
ULK2
HERPUD1
RRAGA
PLPP1
RPS6KB1
ATP6V1B2
MTMR2
TMEM55B
EIF2AK1
NCK2
AARS2
PCYT1A
GARS
GPD2
HBEGF
Log FC
-3
3